UNIVERSITÀ DEGLI STUDI DI PADOVA

DIPARTIMENTO DI INGEGNERIA DELL'INFORMAZIONE

DEPARTMENT OF INFORMATION ENGINEERING

MASTER'S DEGREE IN ICT FOR INTERNET AND MULTIMEDIA

"SIMILAR WIRES, DIFFERENT FIRES: RECONSIDERING THE LINK BETWEEN RESTING-STATE FUNCTIONAL CONNECTIVITY AND PSYCHOPATHIC TRAITS"

Supervisor: Prof. Alessandra Bertoldo

Candidate: Sofiia Tatosh

Student ID
2072547

Co-supervisors: Prof. Stéphane A. De Brito
Dr. Jules R. Dugré
University of Birmingham,
Center for Human Brain Health

ACADEMIC YEAR 2024 – 2025

Graduation date *4 December 2025*

To my beloved grandfather, Mykola, who once (im)patiently taught me the multiplication table. Today I graduate in an applied field, carrying those early lessons with me. I wish you could see this moment - I know you would be proud.

Abstract

Psychopathy is a multifaceted construct encompassing affective, interpersonal, behavioural, and antisocial traits. Intrinsic brain organization, captured via functional connectivity, is widely used to map brain-behaviour relationships and to characterize the neural underpinnings of psychopathology. Prior work reports associations between psychopathic traits and altered connectivity in the frontoparietal control, default mode, and salience networks. However, current evidence is constrained by small sample sizes and the reliance on Western, Educated, Industrialized, Rich, and Democratic populations. Therefore, cross-cultural predictive modeling is crucial for identifying robust and generalizable biomarkers linked to psychopathic traits.

To address these gaps, I tested whether resting-state functional connectivity (rsFC) predicts psychopathic traits in a non-Western community cohort. Participants (n=97, 52 females, community sample, Japan) completed the Self-Reported Psychopathy Scale-Short Form (SRP-SF) and underwent structural and resting-state functional magnetic resonance imaging. Connectome-based Predictive Modeling (CPM) with cross-validation was applied, and generalizability was evaluated in an independent dataset (n=107, 68 females, community sample, Germany).

Across both cohorts, CPM failed to predict psychopathy scores out-of-sample, regardless of model parameters, psychopathic subdimensions, or potential sex differences. Post-hoc analyses indicated, however, that individuals with higher psychopathy scores exhibited more homogeneous rsFC patterns, whereas those with lower scores showed greater variability, suggesting score-dependent heterogeneity in brain-behaviour mapping. These findings highlight key challenges for predictive modeling and point to several future directions, including larger samples, the use of non-linear models, and potentially a shift toward individual-level connectome characterization to better capture heterogeneous neural substrates of similar behavioural phenotypes.

Abstract (Italiano)

La psicopatia è un costrutto multifattoriale che comprende tratti affettivi, interpersonali, comportamentali e antisociali. L'organizzazione intrinseca del cervello, misurata tramite la connettività funzionale, è ampiamente utilizzata per mappare le relazioni tra cervello e comportamento e per caratterizzare le basi neurali della psicopatologia. Studi precedenti hanno riportato associazioni tra tratti psicopatici e connettività alterata nelle reti di controllo frontoparietali, default mode e di salienza. Tuttavia, l' evidenza attuale e' limitata da dimensioni campionarie ridotte e da una forte dipendenza da popolazioni WEIRD (Western, Educated, Industrialized, Rich, Democratic). Pertanto, lo sviluppo di modelli predittivi cross-culturali è cruciale per identificare biomarcatori robusti e generalizzabili associati ai tratti psicopatici. Per affrontare queste lacune, abbiamo testato se la connettività funzionale a riposo (rsFC) predice i tratti psicopatici in un gruppo comunitario non occidentale. I partecipanti (n=97, 52 donne, campione di comunità, Giappone) hanno completato la Self-Reported Psychopathy Scale – Short Form (SRP-SF) e sono stati sottoposti a risonanza magnetica strutturale e funzionale a riposo. È stata applicata la Connectome-based Predictive Modeling (CPM) con cross-validazione e la generalizzabilità è stata valutata in un dataset indipendente (n=107, 68 donne, campione di comunità, Germania). In entrambe le coorti, la CPM non è riuscita a predire i punteggi di psicopatia out-of-sample, indipendentemente dai parametri del modello, dalle sottodimensioni psicopatiche o da potenziali differenze di sesso. Le analisi post hoc hanno tuttavia indicato che gli individui con punteggi di psicopatia più elevati presentavano pattern di rsFC più omogenei, mentre quelli con punteggi più bassi mostravano una maggiore variabilità, suggerendo un'eterogeneità dipendente dal punteggio nelle relazioni cervello–comportamento. Questi risultati evidenziano sfide cruciali per la modellizzazione predittiva e indicano diverse direzioni future, tra cui l'impiego di campioni più ampi, l'uso di modelli non lineari e, potenzialmente, un passaggio verso una caratterizzazione del connettoma a livello individuale, al fine di cogliere meglio substrati neurali eterogenei alla base di fenotipi comportamentali simili.

Contents

Listing of figures

Listing of tables

Listing of acronyms

BWAS . . . . . Brain-Wide Association Studies

CPM . . . . . Connectome-Based Predictive Modelling

DMN . . . . . Default Mode Network

ENIGMA-ASB ENIGMA Antisocial Behavior Working Group

FC . . . . . Functional Connectivity

FDR . . . . . False Discovery Rate

FPN . . . . . Frontoparietal Control Network

fMRI . . . . . Functional Magnetic Resonance Imaging

IS-RSA . . . . . Inter-Subject Representational Similarity Analysis

MAE . . . . . Mean Absolute Error

MRI . . . . . Magnetic Resonance Imaging

NBS . . . . . Network-Based Statistics

NBS-CPM . . . . . Network-Based Statistics Connectome-Based Predictive Modelling

NN . . . . . Nearest-Neighbour Model

pFDR . . . . . False Discovery Rate–Corrected p-Value

ROI . . . . . Region of Interest

rsFC . . . . . Resting-State Functional Connectivity

SD3 . . . . . Short Dark Triad

SN . . . . . Salience Network

SRP-SF . . . . . Self-Report Psychopathy Scale – Short Form

sMRI . . . . . Structural Magnetic Resonance Imaging

WEIRD . . . . . Western, Educated, Industrialized, Rich and Democratic

1

Introduction

The fascination with "psychopathy" in the media is gaining more and more popularity over time. From TV shows to true crime podcasts, it attracts public attention by combining danger, morality, and mystery. On screen, characters are often manipulative, extreme, cold, and hyper-competent, which is entertaining to some extent, but provides a misrepresentation of this entity. Indeed, most dramatic portrayals of psychopathic individuals often diverge from how clinical science describes them. In reality, where the media presents psychopathy as usually related to crime, violence, and murder, researchers and clinicians consider it a severe personality disorder that can be found to varying degrees, even in non-criminal populations. Early documented observations of psychopathy originated from the clinical work of Hervey Cleckley, as outlined in "The Mask of Sanity" (1941). Cleckley described psychopathic individuals as those who presented a convincing "mask" of normality, high intelligence, and charm, which in turn concealed a profound lack in internal emotional experience, empathy, and social responsibility[1]. Through decades of research, involving clinical interviews with incarcerated populations, the Hare Psychopathy Checklist assessment tool was developed, which became the gold standard for research and forensic settings. Nowadays, it is frequently operationalized as a four-facet model, which organizes the traits into two broad domains. The first one represents interpersonal and affective facets that reflect limited empathy, shallow affect, and a tendency to manipulate others. The other is characterized by impulsivity and chronic disregard for rules and spans lifestyle and antisocial facets[2]. Thus, psychopathy is not a unitary entity, but a multidimensional phenotype

that varies across people and contexts.

While the aforementioned traits are relatively uncommon in the general community, they are associated with significant concentrated harms in specific settings, including the criminal justice system. In fact, 10 – 25% of incarcerated individuals exhibit elevated psychopathy levels[3], [4], [5], whereas the prevalence in community samples is estimated to be ~ 2%[6]. This high concentration of individuals with psychopathy among carceral and forensic settings can be partially explained by an existing overlap with Antisocial Personality Disorder (ASPD), a diagnosis defined by a recurring pattern of antisocial behaviors like aggression, deceit, law-breaking, and violation of others' rights. About 80 – 90% of individuals meeting diagnostic criteria for psychopathy, also meet diagnostic criteria for ASPD, but only 25 – 40% of those with ASPD would qualify for a diagnosis of psychopathy[2]. Taking this in consideration, it is important to acknowledge the comorbidity of psychopathy and ASPD, as it reveals that the combination of both is strongly linked to a higher risk of severe violence and related harms[7].

The consequences of psychopathy are indeed severe. Longitudinal studies confirm that individuals with psychopathy are at risk for a persistent, life-course pattern of adverse outcomes, extending to instrumentally violent offending and recidivism[8], rearrest[9], and high long-term mortality[10]. Furthermore, the lifestyle and antisocial facets of the personality disorder are associated with comorbid substance use disorders that take onset during early adulthood[11] and may predict substance-related reoffence[12]. The societal burden is tremendous as well, as psychopathy causes substantial harm to victims. For instance, intimate partners of individuals with psychopathic traits report various forms of abuse and emotional, behavioral, cognitive, and interpersonal difficulties[13]. Psychopathic traits also appear adept at identifying and manipulating vulnerable victims, which increases the risk concerning emotional and physical safety[2]. Additionally, a recent cost-of-illness analysis estimated that crime attributable to psychopathic personality disorder totals $245 – $1592 billion per year in the United States, and $12 – $53 billion in Canada[14]. In England and Wales, the annual economic and social cost of reoffending (a domain for which psychopathy is a substantial risk factor) has been valued at £18.1 billion in official estimates[15]. This extensive societal and economic impact highlight the need for a thorough scientific understanding of the problem. To develop effective interventions, it is necessary to better understand the core mechanisms underlying this persistent and harmful behavior.

The pursuit of this objective marked a crucial turning point for the field, shifting research focus to specific neural systems. Cognitive functions such as flexible updating, impulse control, and learning from punishment were already known to be governed by the prefrontal cortex (PFC)[16], [17], [18]. A compelling line of evidence regarding the PFC involvement in

psychopathy-like behavior comes from classic human lesion studies. One of the most prominent cases is that of Phineas Gage, whose injury to the left frontal lobe had a devastating effect on personality and social behavior. After the injury, Gage displayed aggressiveness, impatience, impulsivity, and irritability, as well as poor social judgment [19]. Other studies showed that damage to the orbitofrontal and ventromedial prefrontal regions was often followed by disinhibition, poor judgment, and blunted affect and reduced empathy [20], [21]. Since the behavioral changes closely resembled what was known about developmental psychopathy, and at the same time, it was critical to disentangle the two conditions, as their origins are fundamentally different, the lesion-induced phenomenon was termed "pseudopsychopathy"[20]. The former typically has an early onset and is thought to result from a complex interplay between genetic and environmental factors, as well as from more subtle, atypical brain development in key circuits[2]. Even though the two are not identical, the lesion findings were a powerful discovery that provided the first causal evidence that damage to the PFC could produce a clinical presentation resembling developmental psychopathy. These observations led researchers to investigate further the role of prefrontal regions using neuroimaging techniques [22].

To unravel the complex etiology of psychopathy, researchers have formulated various theoretical models. These can be broadly categorized into emotion-based perspectives, such as the low fear hypothesis[23], [24], and fearlessness models[25]; cognitive-based perspectives, including the response modulation hypothesis[26] and the attention bottleneck theory[27]; and neural-based perspectives, such as the somatic marker hypothesis[28], paralimbic dysfunction[29], and the integrated emotion system[30].

During the first wave of neuroimaging studies in the field, the question that arose was whether the PFC of individuals with psychopathic traits differs from the PFC of typically developing controls. Early structural Magnetic Resonance Imaging (sMRI) studies examining brain volume and shape provided the first evidence in support of that hypothesis. Compared to the control group, individuals with ASPD showed grey matter volume in the PFC, the area identified in the lesion studies[31]. Additionally, studies employing Positron Emission Tomography (PET), which measures baseline brain metabolism, found atypical reductions in activity in the same frontal regions in samples of murderers [32], [33]. The breakthrough, however, was the use of functional MRI (fMRI), which enabled researchers to measure a signal as a proxy for brain activity during a task. Study participants could now perform emotional or decision-making tasks directly in the scanner, which facilitated the establishment of relationships between brain activation and behavior. Early fMRI work on criminal psychopaths not only provided additional evidence of hyperactivation of PFC during affective processing, but also introduced another key region, the amygdala, a core

hub for emotion and salience[34]. Later, a new method, Diffusion-Weighted Imaging (DWI), emerged to offer a way to measure the integrity of the brain's white matter tracts. Researchers found that the tracts connecting the PFC and amygdala were compromised in individuals with psychopathy[35]. These studies provided support to models such as Blair's amygdala-vmPFC dysfunction[36] and Kiehl's paralimbic dysfunction hypothesis[37], which reflects a disruption of prefrontal-amygdala communication rather than purely a prefrontal deficit.

More recently, the field shifted from assessing single regions to analyzing how they communicate with each other and began using resting-state fMRI (rs-fMRI) to measure functional connectivity - the way brain regions communicate at rest. Unlike task-based studies that probe neural activity in response to stimuli, resting-state fMRI characterizes the organization of brain regions without explicit cognitive demands, that may be a more accurate representation of the long-term affective and social characteristics of psychopathy. Resting-state fMRI work has revealed that the brain alterations in psychopathy are not limited to the fronto-limbic system but involve large-scale networks, such as the Default Mode Network (DMN), Frontoparietal Network (FPN), and Salience Network (SN) [38], [39], [40]. However, the findings remain heterogeneous, as per recent meta-analytical evidence that indicates mixed, method-dependent effects[41], [42], [43], [44]. Consequently, this area requires more rigorous attention to clarify those inconsistencies and to better understand the neural correlates of the disorder.

While the network approach, built on decades of group-level data, reflects the current consensus, a substantial gap remains between group-level data and their translation to individual-level clinical application. As the literature expanded, inconsistencies across this body of work became apparent. One major contribution to this lack of replication is that studies have relied on small samples, likely overestimating effects and making findings unstable. This has led to the realization that, despite significant progress, psychiatric neuroimaging results still have limited direct clinical use[45]. Notably, these challenges are not unique to psychopathy, but instead they arise across human neuroscience [46].

Since the sample problem is not just about size, but about composition, another fundamental barrier to generalizability is *who* is being studied. The vast majority of our scientific knowledge in psychology and neuroscience is built on a small, highly unrepresentative subset of communities: Western, Educated, Industrialized, Rich, and Democratic (WEIRD) populations[47]. Demographic reporting in neuroimaging, for example, is often incomplete, and samples are rarely representative of the broader populations. A decade-long systematic review found inconsistent reporting of race and ethnicity, while many MRI studies still omit basic participant demographics[48]. Conclusions drawn from only WEIRD-dominated datasets might not gen-

eralise to different cultures or demographics, thereby limiting the potential translational impact of the findings. Therefore, this is not just an equity issue; it is a critical scientific requirement to address representation in neuroscience to produce results generalizable beyond the narrow WEIRD samples[49].

This study directly examines the cross-cultural generalisability of psychopathy. Rather than relying solely on WEIRD samples, it investigates brain–behaviour associations in two community cohorts from distinct cultural contexts—Japan and Germany. The central aim is to test whether previously reported links between brain connectivity and psychopathic traits replicate and extend across cultures. Using modern predictive modelling techniques, I tested whether brain connectivity during rest can successfully predict inter-individual variability in psychopathic traits. This approach allows us to ask whether the neural mechanisms that are thought to be cross-culturally consistent are, in fact, robust across populations. Overall, this thesis re-evaluates the potential of resting-state functional connectivity as a robust and generalizable predictive marker of psychopathic traits.

2

Background

2.1 Historical Perspective on Measurement of Psychopathy

2.1.1 The Clinical Construct: PCL-R and the four-facet model

Psychopathy is a personality disorder characterized by a set of affective, interpersonal, behavioral, and antisocial traits such as shallow affect, lack of empathy, grandiosity, impulsivity, manipulativeness, poor decision-making, parasitic lifestyle, and disregard for social norms, including criminal versatility[2], [50]. The modern scientific understanding of psychopathy is built upon the foundational clinical observations of an American psychiatrist, Hervey Cleckley. His seminal work, "The Mask of Sanity" (1941), provided one of the most influential and comprehensive descriptive profiles of the disorder[51]. In later editions of the work, Cleckley outlined 16 clinical criteria that together summarize the characteristics of a psychopath, which included lack of empathy and remorse, superficial charm, and poor judgment, as well as low anxiety, absence of neurotic symptoms, and a history free of suicide attempts [1]. While the described portrait provided the essentials for understanding psychopathy, it lacked standardization and objective scoring, which are needed for rigorous clinical applications. This gap was later filled by Dr. Robert D. Hare, a forensic psychologist who developed the Psychopathy Checklist based on Cleckley's construct[52]. The new assessment instrument, namely, the Hare Psychopathy Checklist (PCL), was designed to quantify psychopathic traits, specifically for use in prisons[52].

The psychopathy checklist, originally introduced as a 22-item rating scale, was later refined into the Hare Psychopathy Checklist-Revised (PCL-R) and has become the gold standard for assessing psychopathy in both clinical and offender populations. The refinements included the removal of two poorly performing items (due to their low correlations with the total score and being difficult to score) and the clarification of scoring criteria. The PCL-R is a 20-item clinical assessment tool created to measure the presence and severity of psychopathic traits[53]. It is essential to note that the PCL-R is not a self-report questionnaire, but rather a semi-structured interview that can only be administered by a trained professional. The administration process is extensive, involving mandatory specialist training, access to records documenting the assessed individual's lifetime behavior, and an interview that typically lasts up to 3 hours [2]. The collateral file review, which includes examining criminal records, medical and school records, and employment history, is an essential part of the process, as it allows the clinician to corroborate the subject's claims and self-presentation against objective life-history data. Based on the combined evidence from the interview and records review, the professional scores each of the 20 items on a 3-point scale $(0, 1, 2)$. The total score ranges from 0 to 40, with higher values indicating greater severity of psychopathic traits[53]. In forensic practice, PCL-R scores are often interpreted using thresholds: a total score cut-off of 30 is typically used in North America, whereas lower thresholds around 25 are commonly adopted in many European jurisdictions to classify an individual as psychopathic[54]. This use of cut-offs reflects a categorical view of psychopathy, where individuals are treated as either psychopathic or non-psychopathic. This profile, however, is not monolithic; it is composed of distinct groups of characteristics. A key feature of PCL-R is that its items form a coherent hierarchical structure.

Initially, factor analyses of the PCL-R items identified a two-factor model that divided psychopathy into two distinct but interrelated components[55]. Factor 1 captures the affective and interpersonal deficits such as callousness, grandiosity, manipulation, and tactical exploitation of others. Factor 2, on the other hand, reflects an antisocial, impulsive lifestyle including irresponsibility, criminal versatility, and chronic rule-breaking. This two-factor structure was pivotal, as it highlighted that individuals could differ in their relative elevations on these components[56]. For instance, it became possible to identify individuals with elevated interpersonal affective features but a relative absence of persistent antisocial behavior, or vice versa, who were still classified as psychopathic.

Over time, further research and concept refinements demonstrated that psychopathy is better captured by a hierarchical four-facet model with facets forming two broader, higher-order factors[57]. This model divides the 20 items into four specific facets: interpersonal (e.g., super-

ficial charm, grandiose sense of self-worth, manipulation of others), affective (e.g., lack of guilt, shallow affect, lack of empathy), lifestyle (e.g., parasitic lifestyle, impulsivity, irresponsibility), and antisocial (e.g., criminal, aggressive behavior, habitual rule breaking)[57] (see Figure 2.1). This four-facet structure provides a coherent map of all features of psychopathy, from its internal affective-interpersonal core to its external lifestyle-antisocial expressions.

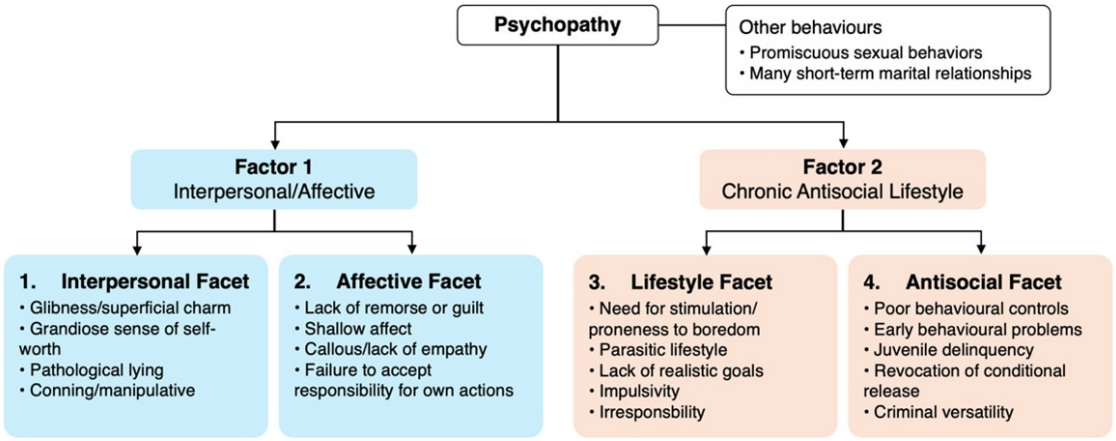

Figure 2.1: Two-factor, four-facet model of psychopathy as assessed in the PCL-R. Factor 1 comprises the interpersonal and affective facets; Factor 2 comprises the lifestyle and antisocial facets.

Although the hierarchical model has been highly influential in clinical and forensic work, the PCL-R is still usually applied in a categorical way, with score cut-offs defining psychopathic vs. non-psychopathic individuals[54]. By contrast, studies that explicitly tested whether psychopathy is categorical or continuous, generally support a dimensional view, indicating that psychopathic traits vary in degree across the population[58], [59]. In line with this, more recent work has shifted towards dimensional assessment, using self-reported instruments such as the Self-Report Psychopathy Scale (SRP-SF)[60], which is used in this thesis. It was developed as a self-report extension of the PCL-R for use outside strictly forensic settings.

From a practical perspective, the PCL-R's strengths in a forensic context are also its greatest limitations for other types of research. The "gold standard" is, in fact, time-intensive, expensive, and impractical for use in the large-scale community samples. These limitations, together with the move toward dimensional models, motivated the development of alternative self-report measures that capture the four-facet structure of psychopathy without the administrative burden of the PCL-R.

2.1.2 Measuring Psychopathic Traits in Community Samples

Self-report questionnaires emerged as alternative assessment tools aimed at understanding how psychopathic traits are distributed and expressed in non-forensic community samples[61]. These

are practical instruments where participants respond to a series of statements about their own personality, feelings, and behaviors, typically by rating their agreement on a Likert-type scale (commonly 4- or 5-point, depending on the instrument). The primary advantages of this approach are efficiency and scalability. Self-report measures are highly cost-effective, can be administered to hundreds or even thousands of participants at once, and do not require a trained professional for administration[62].

However, despite these clear practical advantages, the question of the validity of self-report measures emerges[63]. Psychopathy, by its very definition, includes traits like pathological lying, manipulativeness, and a grandiose sense of self-worth. How, then, can researchers rely on the accuracy of self-reports from an individual exhibiting these traits? While this is a serious concern, two primary lines of evidence support the use of self-report measures in this context. First, the assessment context has a significant influence on responses. Self-reports of participants tested in a high-stakes environment (e.g., forensic) may be influenced by a strong external incentive to "fake good" (or bad, depending on the desired outcome). In contrast, a typical community research study involves voluntary participation with no personal stakes tied to the outcome, which minimizes motivation for deliberate lying[64]. Second, and most importantly, self-report tools have undergone extensive empirical validation. This work has shown significant correlations with a range of objective criteria, including PCL-R scores, in studies where both measures were administered[65], behavioral outcomes[66], and informant reports[67]. Therefore, while researchers must remain critical, the evidence suggests that self-report questionnaires are a valid and reliable method for measuring psychopathic traits, provided they are used in the appropriate context.

There are several widely-used self-report instruments that reflect overlapping theoretical conceptualization of psychopathy, including the Self-Report Psychopathy scales (SRP)[68], the Psychopathic Personality Inventory-Revised (PPI-R)[69], the Triarchic Psychopathy Measure (TriPM)[70], the Levenson Self-Report Psychopathy Scale (LSRP)[71], the Psychopathic Boldness Scale[72], and the Elemental Psychopathy Assessment (EPA)[73]. In the present thesis, I focus on the SRP Short Form scale and Short Dark Triad[74], which serve as the primary self-report measures of psychopathic traits in the Japanese and German samples, respectively.

2.1.3 The Self-Report Psychopathy Scale

The Self-Report Psychopathy Scale 4th Edition (SRP-4) is designed to be both psychometrically accurate and comprehensive as a self-report measure, with a similar hierarchical structure to

the PCL-R, but suitable for use in community samples. The SRP-4 comprises 64 items, each using a 5-point Likert scale. The SRP-SF items yield a Total psychopathy score and two factor scores (Factor 1 and Factor 2), representing broader dimensions of psychopathic traits. These factors can then be decomposed into four facet scores - interpersonal, affective, lifestyle, and antisocial[68].

Importantly, although SRP factors are overlapping, they show distinct patterns of association with personality traits, symptoms, and behavior[75], [76]. In large student and community samples, the interpersonal-affective facets (Factor 1) are most strongly linked to an antagonistic, low-agreeableness interpersonal style[77] and reduced empathy[78], [79], but show only modest associations with overt antisocial behavior[75]. On the other hand, the lifestyle and antisocial facets (Factor 2) are more clearly tied to impulsivity, rule-breaking, substance use, and other externalizing problems[75], [76], [80]. Meta-analytic work on psychopathy measures further supports these findings by demonstrating that disinhibitory and antisocial dimensions show consistently stronger associations with aggression and externalizing psychopathology than interpersonal-affective traits[81], [82].

Although the 64-item SRP-4 is comprehensive, it still presents a practical limitation. In many large-scale research studies, especially those involving demanding neuroimaging protocols, participants' time is a valuable and limited resource. This created a clear need for an instrument that could strike a balance between psychometric rigor and practical efficiency. Thus, the Self-Report Psychopathy Scale Short Form (SRP-SF) was derived from the full 64-item SRP-4, where 29 items were selected based on their reliability and ability to represent the four primary facets of the original questionnaire effectively[83].

2.1.4 The Dark Triad Model

The Dark Triad (DT) refers to a constellation of three distinct aversive personality traits, such as Narcissism (e.g., lack of empathy, egotism, and dominant personality), Machiavellianism (e.g., strategic, manipulative, and exploitative in achieving personal goals), and Psychopathy (e.g., impulsivity, low empathy, and callousness)[84] (see Figure 2.2). Although these traits possess unique features, they can be grouped under the same "umbrella" because they share a common "dark core" associated with self-serving, manipulative, and often harmful behaviors, all of which are centered around personal benefit at the expense of others[84].

One of the most widely used tools to empirically assess this three-part constellation is the Short Dark Triad (SD3). It consists of 27 items on the self-report questionnaire and maps di-

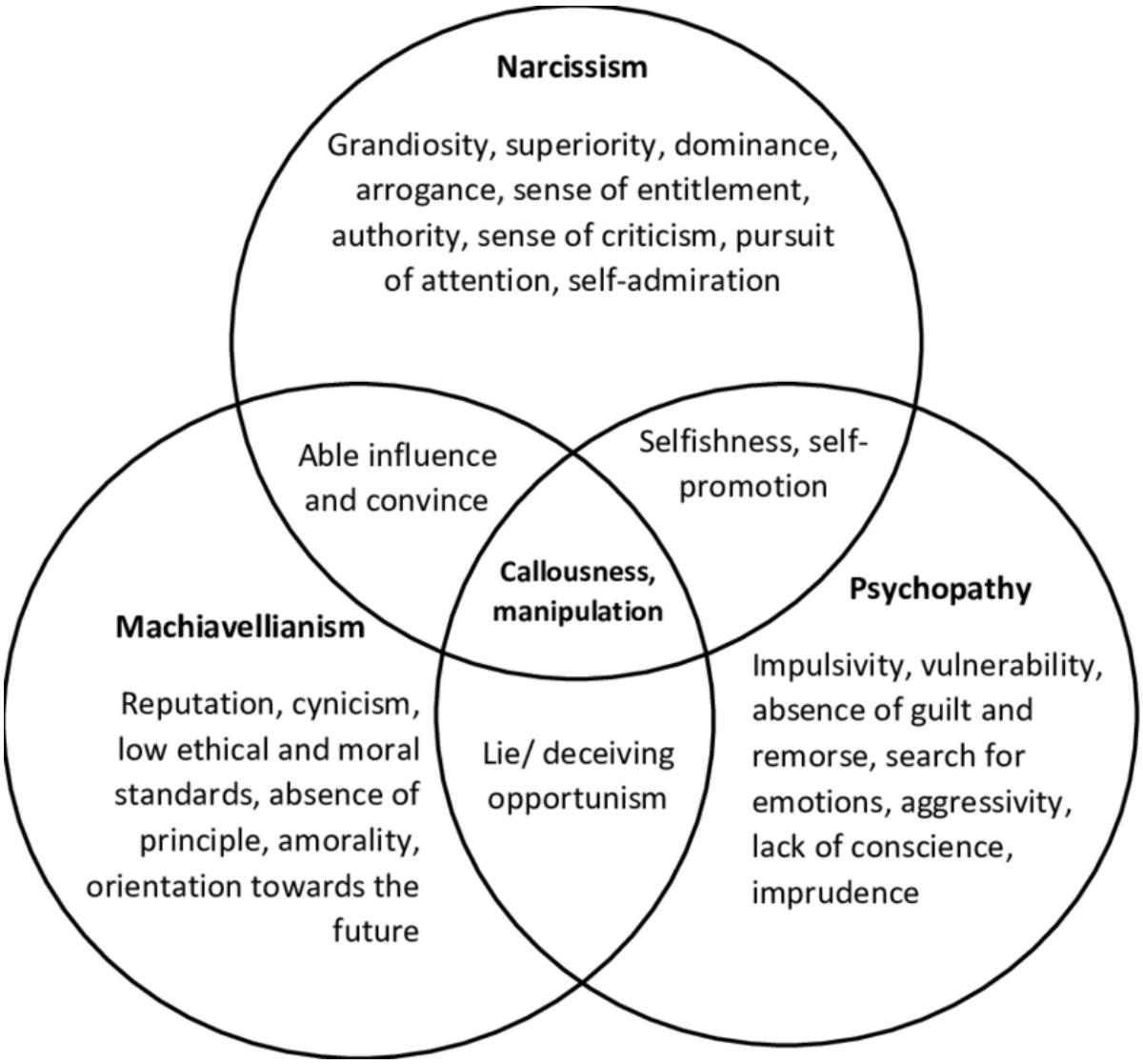

Figure 2.2: The Dark Triad personality traits. A Venn diagram illustrates the distinguishing and shared characteristics of narcissism, machiavellianism, and psychopathy. (D'Souza et al.. 2019)[85]

rectly onto the three core components of the model, with 9 items dedicated to each of the categories. Participants rate their agreement with each given statement on a Likert-type scale from 1 to 5, resulting in scores for each of the three Dark Triad traits[74]. The SD3 subscales generally show acceptable internal consistency and a replicable three-factor structure corresponding to the intended traits, as supported across the original development studies and subsequent validations in various samples[74], [86], [87], [88]. In this thesis, the SD3 questionnaire was used as a psychopathy metric for the German dataset. Thus, it is worth mentioning that the German adaptation of the SD3 has also demonstrated a clear three-factor structure, adequate reliability and validity in large German-speaking samples[89], [90].

2.2 Neurocognitive Profile of Psychopathy

The previous section described psychopathic traits and their assessment with self-report instruments, focusing on the Self-Report Psychopathy Scale - Short Form and the psychopathy subscale of the Short Dark Triad, both used in this thesis. This section provides a brief overview on behavioral and cognitive findings in psychopathic traits.

Importantly, decades of experimental work has shown that higher psychopathic traits (particularly in forensic and high-risk samples) are linked to alterations in emotion, learning, and social decision making. For example, psychopathic offenders show reduced fear conditioning and weaker autonomic responses when neutral cues are paired with aversive outcomes. They display little or no increase in skin conductance and attenuated activation of limbic and frontal brain regions (including the amygdala, insula, and anterior cingulate cortex) during aversive Pavlovian conditioning[91], [92], [93]. In addition, meta-analyses of facial emotion recognition indicate that individuals high in psychopathic traits perform worse at identifying negative expressions across modalities and samples[94], [95]. Reduced physiological and self-reported responses to others' distress, and lower affective empathy, have also been repeatedly documented[96], [97].

Psychopathy has also been linked to atypical reinforcement learning and decision making, especially in relation to punishment. For example, in classic passive-avoidance tasks, psychopathic offenders, despite being punished, continue responding to the stimuli, instead of learning to withhold responses, which indicates impaired learning from negative outcomes[98], [99]. Additionally, behavioral and neuroimaging studies of reversal learning and other reinforcement paradigms similarly report reduced sensitivity to changing punishment or reward contingencies[100], [101].

Another line of work points to differences in moral and empathy processing. Studies indicate

that individuals with higher psychopathic traits are more likely to choose "utilitarian" options in personal moral dilemmas (for example, sacrificing one person to save several others) and are more willing to say that causing others emotional distress is morally acceptable[102], [103], [104]. These findings align with clinical descriptions of shallow affect and diminished guilt and concern for others' suffering in psychopathy[57].

Taken together, this body of work converges on the idea that psychopathy associated with a specific pattern of emotional, learning, and moral/empathetic differences, pointing to particular corresponding dysfunctions in brain systems. Neuroimaging offers a non-invasive way to study these alterations and to quantify both brain's anatomy and functional patterns. In the following sections, I therefore introduce the magnetic resonance imaging methods and functional measures used in this thesis to characterize individual differences in brain organization as a function of psychopathic traits measured by the SRP-SF and SD3 self-report scales.

2.3 Neuroimaging

With the behavioral constructs and their measurements defined, the next step is to describe how the brain systems implicated in psychopathy are measured in vivo. Neuroimaging, and in particular Magnetic Resonance Imaging (MRI), provides the functional data on which the present analyses are based. This chapter introduces the MRI modalities used in this thesis, providing a brief overview of structural MRI and focusing on functional MRI and resting-state fMRI. A dedicated subsection on whole-brain functional connectivity is included because these measures form the connectome features that are later used as predictive features of psychopathic traits.

2.3.1 Magnetic Resonance Imaging (MRI)

Magnetic Resonance Imaging (MRI) is a non-invasive imaging technology widely employed in medicine and neuroscience to produce detailed anatomical images of the body, including the brain. Unlike other imaging techniques, such as X-rays or Computed Tomography (CT) scans, it does not use ionizing radiation, meaning patients can be scanned safely and, if necessary, repeatedly, with minimal risk to their health[105]. This makes it a practical and ethically viable tool in modern neuroscience. It also allows researchers to move beyond clinical case studies and investigate brain structure and function in the large, healthy, non-clinical community samples.

At its core, the MRI scanner is a giant, incredibly powerful magnet. Its strength is measured in units called Tesla (T). The scanners used in modern clinical and research settings typically

operate at 1.5T or 3T, whereas some advanced research scanners can reach 7T or higher[106]. For comparison, the Earth's magnetic field, which guides a compass, is approximately 0.00005T; a standard refrigerator magnet is around 0.01T. A 3T scanner, common in research and clinical imaging, generates a magnetic field roughly ~ 60000 times stronger than the Earth's.

Although MRI does not emit ionizing radiation, its strong magnetic field extends beyond the machine and exerts power on magnetizable objects. Thus, there are strict rules and a predefined set of precautions that every patient, physician, and general scanner room visitor needs to comply with. When undergoing an MRI scan, participants are asked to complete a questionnaire covering all possible aspects that might pose a risk to them in the scanner, such as iron implants, pacemakers, or metal fragments in and on the body. It is also recommended to avoid MRI scanning as a precaution if participants have noise sensitivity, claustrophobia, or are pregnant (especially in the first trimester)[107]. With all rigorous precautions in place, MRI is considered one of the safest tools in neuroimaging.

2.3.2 Functional MRI

In MRI studies, it is standard to acquire a high-resolution structural (T1-weighted) scan before any functional imaging. Structural MRI provides a detailed 3D image of the brain's anatomy that clearly separates grey matter, white matter, and cerebrospinal fluid. In the present study, the structural images are used as an anatomical reference: functional data are aligned to it, and the structural scan is parcellated so that time series can later be extracted from predefined regions.

By contrast, functional Magnetic Resonance Imaging (fMRI) is designed to move beyond anatomy and measure the physiological changes associated with brain activity over time. While an sMRI scan acquires a single, high-resolution anatomical image over several minutes, an fMRI scan must capture the entire brain much more rapidly and repeatedly to track the changes in activation[106]. To achieve this speed, fMRI sacrifices spatial resolution (the level of detail) to gain high temporal resolution (the ability to detect changes quickly). Therefore, a single fMRI "run" does not produce a single image; it yields a time series, a collection of hundreds of sequential 3D images, known as volumes. This is precisely what allows researchers to track the signal changes in any specific brain region from one moment to the next[106], [108].

fMRI measures an indirect proxy of neuronal activity, known as the Blood-Oxygen-Level-Dependent (BOLD) signal[109]. This technique relies on the different magnetic properties of hemoglobin, specifically deoxygenated and oxygenated hemoglobin, where the former is paramagnetic, meaning it acts like a tiny magnet that distorts the local magnetic field, and the latter

is diamagnetic, or magnetically neutral[108], [109]. In a resting state, brain regions have a baseline concentration of deoxygenated hemoglobin. When a region becomes active, local blood flow increases, resulting in an oversupply of oxygenated blood to the area. Having diamagnetic blood displacing the paramagnetic deoxygenated hemoglobin, the local magnetic field becomes more uniform. The fMRI scanner, being highly sensitive to changes, detects increased uniformity as a slight increase in the signal[108]. Therefore, the BOLD signal that we measure is not the neural activity itself; however, an increase in the BOLD signal reflects a decrease in local deoxygenated hemoglobin, which is a reliable proxy for a recent increase in neural activity[110].

2.3.3 Task-based fMRI

Historically, the field of functional neuroimaging was primarily dominated by task-based fMRI, where researchers measure the BOLD signal changes evoked by a specific external stimulus[111]. In a typical task-based experiment, participants perform a controlled cognitive or affective task, such as, for example, viewing emotional faces, making moral judgements, or learning from reward or punishment, while BOLD responses are measured to track condition-specific changes in neural activity[112]. Consequently, task-based fMRI has been widely used in psychopathy research, with paradigms that target fear and threat processing, reward and punishment learning, empathy, and moral decision-making. It is typically used to test specific hypotheses about which psychological processes and brain regions are altered in individuals with high psychopathic traits[113], [114].

Many early task-based fMRI studies reported reduced amygdala responses to fearful or distressing cues, atypical activation of ventromedial prefrontal cortex (vmPFC), anterior cingulate cortex, and insula during moral or affective tasks in individuals with elevated psychopathic traits[96], [115], [116]. However, recent systematic reviews and meta-analyses have shown that functional findings in psychopathy are in fact quite heterogeneous, reporting mixed patterns of hypo- and hyper-activation across limbic and prefrontal regions, and a large proportion of individual studies have also reported null or non-robust amygdala effects[44], [117], [118], [119].

One of the advantages of task-based fMRI is the ability to control the experiment by manipulating stimuli and conditions, allowing researchers to link differences in brain activation to specific cognitive or affective processes[114]. However, this method heavily depends on the task design and only measures the momentary reaction to a given stimulus, disregarding the long-term neural activity patterns outside of task contexts. Additionally, in psychopathy research, the diversity of paradigms, frequent reliance on region-of-interest analyses, and focus on single

domains (e.g., only fear, or only moral judgment) has contributed to heterogeneous and only partly replicable activation maps across studies[43], [117], [119]. Together, these constraints have motivated the increase in use of resting-state approaches as a complementary tool to study brain function in psychiatric disorders.

2.3.4 Resting-state fMRI

A paradigm shift began with the seminal work of Biswal and colleagues (1995)[120], who acquired and analyzed fMRI data from participants at rest, without them performing any task. The authors observed spontaneous, low-frequency (< 0.1 Hz) BOLD signal fluctuations in the sensorimotor cortex that were highly synchronized with fluctuations in other motor-related regions. This was the first empirical evidence that even in the absence of an explicit task, the brain is highly active[111], and subsequent work further proved that the brain consumes a fair amount of its metabolic resources[121]. Resting-state fMRI offers a robust, data-driven approach for analyzing the brain's functional organization, enabling the investigation of the neural correlates of various psychiatric and neurological disorders[122].

Functional Connectivity

The central inference of resting-state fMRI is that if two brain regions operate together as part of a network, their spontaneous activity is synchronized over time. This concept relies on the definition of Functional Connectivity (FC), which is a temporal correlation between spatially distinct neurophysiological signals[123]. Even in the absence of an explicit task, if BOLD signals from two different areas are synchronized, it is inferred that they are functionally connected[120]. To quantify functional connectivity, the brain is first segmented into a finite set of "nodes". Sometimes, a "node" corresponds to a single voxel in the fMRI volume. However, more commonly, a brain atlas, or parcellation, is used to divide a brain into regions of interest (ROIs) based on anatomical landmarks or functional boundaries[124], [125]. After applying such a parcellation, a representative time series is extracted for each node. This is typically done by averaging the BOLD time series of all voxels within that parcel[126]. Finally, pairwise correlation between all node time series is computed to generate a whole-brain connectivity matrix (size $N \times N$), often referred to as the functional connectome[127].

Importantly, the process of creating a connectome cannot be applied directly to the "raw" BOLD time series, as the data are heavily influenced by noise from non-neural sources such as head motion, respiration, cardiac pulsation, and scanner drift[128], [129]. Therefore, before any

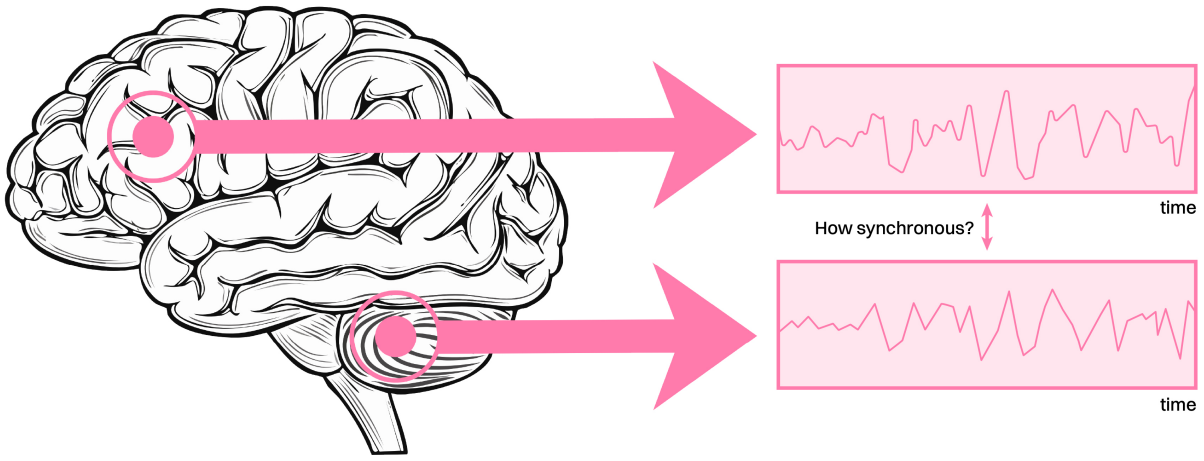

Figure 2.3: Schematic illustration of functional connectivity. Activity time series are extracted from two spatially distinct regions, and the degree of synchrony between their signals over time (e.g., correlation) is used as an index of their functional connectivity.

connectivity analysis is performed, the data must undergo rigorous preprocessing (see Section 3) and data quality control to remove these artifacts and standardize data across subjects[130]. Once preprocessing is complete, multiple analytical approaches can be used depending on the research question. One of the most established methods is seed-based correlation analysis, where a single ROI (or seed) is selected based on an a priori hypothesis. The mean BOLD time series from this seed is then correlated with the time series of every other voxel or region across the brain. The result is a whole-brain statistical map that illustrates the specific network of regions functionally connected with the predefined seed[131]. Alternatively, functional connectome analysis can be approached from a graph theory perspective, where the connectivity matrix is perceived as a graph composed of N nodes (brain regions) and E weighted edges (correlation values). Applying graph theory allows researchers to characterize the brain's global topology, including measures such as efficiency, modularity, and centrality, which capture how effectively information is integrated and segregated across large-scale networks[132].

Large-scale Resting-state Brain Networks

Years of research on functional connectivity have revealed a set of large-scale, reproducible Resting-State Networks (RSNs) in which spatially distributed brain regions exhibit synchronized low-frequency BOLD fluctuations even when no task is performed[133]. The spatial organization of these networks closely parallels co-activation patterns observed during diverse cognitive domains in task-based fMRI, indicating that the same systems engaged during tasks remain

intrinsically coordinated at rest[134]. Beyond primary sensory and motor networks, such as visual, somatomotor, language, and attention networks, three higher-order ("core") RSNs have received particular attention in psychopathology research: the Default Mode Network (DMN), Salience Network (SN), and Frontoparietal Network (FPN), also known as Central Executive Network (CEN)[135].

The Default Mode Network is a distributed set of midline and lateral association regions that includes the medial prefrontal cortex (mPFC), posterior cingulate cortex (PCC) and precuneus, bilateral inferior parietal lobules/angular gyri, lateral temporal cortex, and medial temporal lobe structures such as the hippocampal formation[136] (see Figure 2.4). Initially identified through its task-related deactivation, the DMN shows relatively higher activity at rest and during internally focused thought[137]. Converging evidence links DMN activity to self-referential processing, autobiographical memory, imagining the future, and social-cognitive operations like mentalizing and perspective taking, as shown in task-based fMRI studies where these regions are engaged during self-judgement, theory-of-mind, and moral or social evaluation tasks[138], [139].

The Salience Network, also often referred to as the ventral attention network, has cortical hubs in the anterior insula and dorsal anterior cingulate / mid-cingulate cortex, and extends to fronto-insular, lateral prefrontal, and inferior parietal areas, as well as subcortical regions including the amygdala, ventral striatum, and mediodorsal thalamus[140] (see Figure 2.4). This network integrates interoceptive, affective, and cognitive information to detect and prioritize salient stimuli[141], [142].

The Frontoparietal Network, also called the frontoparietal control or central executive network, comprises lateral prefrontal areas (including dorsolateral and middle frontal gyri and inferior frontal junction) together with posterior parietal regions[143], [144] (see Figure 2.4). In contrast to DMN, which is a network known for its activation during rest, meta-analytic work identifies this network as a core cognitive control system, co-activated across diverse executive tasks[145]. Functionally, the FPN supports goal-directed behavior by maintaining and updating task rules, manipulating information in working memory, and implementing flexible adjustments of behavior[144], [146].

Importantly, these networks do not operate in isolation. They dynamically interact with each other to regulate the balance between internally focused and externally directed cognition, allowing for flexible adaptation to changing environmental demands [135]. For example, SN plays a critical role in mediating dynamic switching between the DMN and FPN to guide behavior according to contextual demands[135], [148]. Meta-analytic work has shown that dis-

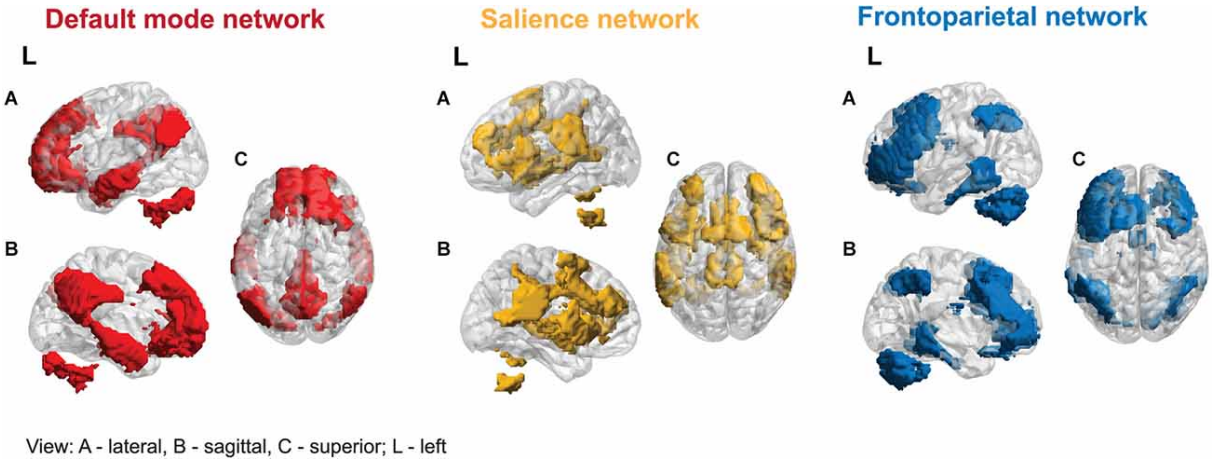

Figure 2.4: Brain surface renderings of the three canonical large-scale functional networks: the default mode network (DMN, red), salience network (SN, yellow), and frontoparietal network (FPN, blue). For each network, panels show lateral (A), sagittal (B), and superior (C) views of the left hemisphere (L) (Schimmelpfennig et al. (2023)[147]).

ruptions within or between these three core networks are common across psychiatric conditions. For instance, the studies found hyperconnectivity within DMN and hypoconnectivity within FPN in depression[149], abnormal SN activity in psychosis[150], and impaired FPN integrity in attention-deficit/hyperactivity disorder (ADHD)[151].

These findings highlight that large-scale resting-state networks such as the DMN, SN, and FPN provide a useful basis for studying psychopathology, because their connectivity at rest reflects stable, trait-like aspects of functional brain organization that differ across individuals. Since psychopathy is characterized by alterations in the functions (see Subsection 2.2) closely associated with default mode, salience, and frontoparietal networks, this motivates a question of the role of connectivity between and within these networks. Therefore, the next section reviews resting-state connectivity findings in psychopathy.

Resting-state Functional Connectivity Findings in Psychopathy

Early neuroimaging work in psychopathy was dominated mainly by hypotheses about the implications of the amygdala and prefrontal cortex (PFC)[37], [96]. These early studies drew rationale from lesion cases and task-based paradigms, arguing that deficits observed in psychopathic individuals were traceable to abnormal connectivity between the vmPFC and limbic regions[44]. However, with the development and use of fMRI, researchers have concluded that even at rest, the brain operates as a network or a set of large-scale sub-networks, and these interactions shape individual personality traits [152]. A landmark shift began when fMRI started to be used to map functional connectivity - the correlation of spontaneous BOLD signals between brain regions at rest[120]. Early findings in psychopathy, employing functional connectivity analysis, reported

reduced coupling between the amygdala and vmPFC, which aligns well with emotion regulation theories[153], [154], [155]. For example, Motzkin et al. (2011) compared incarcerated adults with high PCL-R scores to non-psychopathic offenders and found significantly reduced resting-state functional connectivity between the amygdala and vmPFC (as well as between vmPFC and medial parietal cortex)[154]. However, with the field moving toward larger datasets, the picture began to blur.

With the increasing popularity of large-scale networks as a unit of analysis in neuroscience, Philippi et al. (2015) investigated whether psychopathy is related to connectivity among three "core" cortical networks - DMN, SN, and FPN [135] - at rest. In a sample of 155 adult male inmates, they found that psychopathy severity was associated with reduced functional connectivity within the frontoparietal control network and between the frontoparietal and cingulo-opercular networks, specifically between a right intraparietal sulcus node of the FPN and bilateral dorsal ACC in the CON, as well as the right precuneus within the FPN. Moreover, the authors found that the PCL-R Factors showed opposing connectivity patterns within the same regions: Factor 1 was linked to decreased cortical connectivity, whereas Factor 2 was linked to increased connectivity in the same networks. This split was especially evident for anterior insula-dACC connectivity[156]. Focusing on subcortical-prefrontal circuits, Korponay et al. (2017) reported that higher psychopathy (Factor 2) was associated with abnormal connectivity between the striatum and the dorsolateral prefrontal cortex and ventral midbrain [157]. Additionally, Factor 2 scores were positively correlated with functional connectivity between several areas of the prefrontal cortex[158]. Overall, these studies suggest that psychopathic traits are linked to altered connectivity between and within frontoparietal, cingulo-opercular, and subcortical-prefrontal circuits, rather than to a single region abnormality. At the same time, they rely on relatively small forensic samples and seed-based analyses of a predefined set of networks and regions, which makes it difficult to characterize how psychopathy relates to whole-brain connectivity patterns.

When analyses have been scaled to whole-brain networks in large forensic cohorts, effects have been found to be more selective. For example, in one of the most comprehensive efforts to examine brain connectivity in psychopathic individuals, Espinoza and colleagues (2018) analyzed resting-state data from 985 incarcerated men and estimated functional connectivity among a set of canonical resting-state networks (using an ICA-based functional network connectivity approach[159]). Surprisingly, psychopathy scores measured by the PCL-R showed only weak and highly selective associations with network connectivity. The study found no significant associations between FNC and the PCL-R Total and Factor 2 scores[160]. The same group

later published a study analysing dynamic connectivity and exploring how networks fluctuate over time. They found no stable, directionally consistent associations for Total and Factor 2 scores[161]. These findings suggest that when sample heterogeneity and multiple comparisons are properly controlled for, abnormal connectivity in psychopathy becomes more subtle.

Subsequent studies began to explore whether this subtlety might be better captured in more specific populations. In female offenders, for instance, it was found that women with higher antisocial and lifestyle scores (Factor 2 of the PCL-R) displayed altered within-network coherence within the default mode and paralimbic networks[162]. In a follow-up study on adolescent girls, using the youth version of the PCL (PCL:YV [163]), the authors found disrupted functional coupling within the DMN and between paralimbic structures; however, no inter- and intra-network connectivity survived correction for multiple comparisons[40]. The findings presented similarities with those in adult women, hinting at a developmental continuity of the disorder.

Together, these studies indicate that the neural correlates of psychopathy might express differently across sexes. The studies also underscored a recurring issue of inconsistency, where effects are often sample-specific, their directionality is reversed across cohorts, and many null results are observed. A major step toward addressing the discrepancies in neuroimaging research on psychopathy was provided by a recent meta-analytic network mapping study [164]. It showed that despite broad spatial variability across individual studies, nearly all reported regions converged within a single distributed "psychopathy network". This constellation overlaps strongly with the default-mode network and subcortex, followed by frontoparietal and ventral attention networks[164].

Methodological Approaches to Resting-State Connectivity

A large part of neuroimaging work on resting-state functional connectivity (including studies focused on psychopathic traits) has relied on standard analysis approaches such as seed-based correlation, ROI-to-ROI analyses, independent component analysis (ICA), and graph-theoretical summaries of network topology[165]. Seed-based analysis, for example, requires a priori selection of a small set of "seed" regions and then correlates their time series with the rest of the brain. ICA, in turn, decomposes data into a set of independent components that are interpreted, usually, as resting-state networks, and analysed accordingly. Finally, graph approaches treat the brain as a set of nodes and edges and quantify graph properties like degree, modularity, or efficiency[165]. Together, these approaches have produced important results about altered connectivity patterns in psychopathy and related antisocial conditions, but at the same time, they

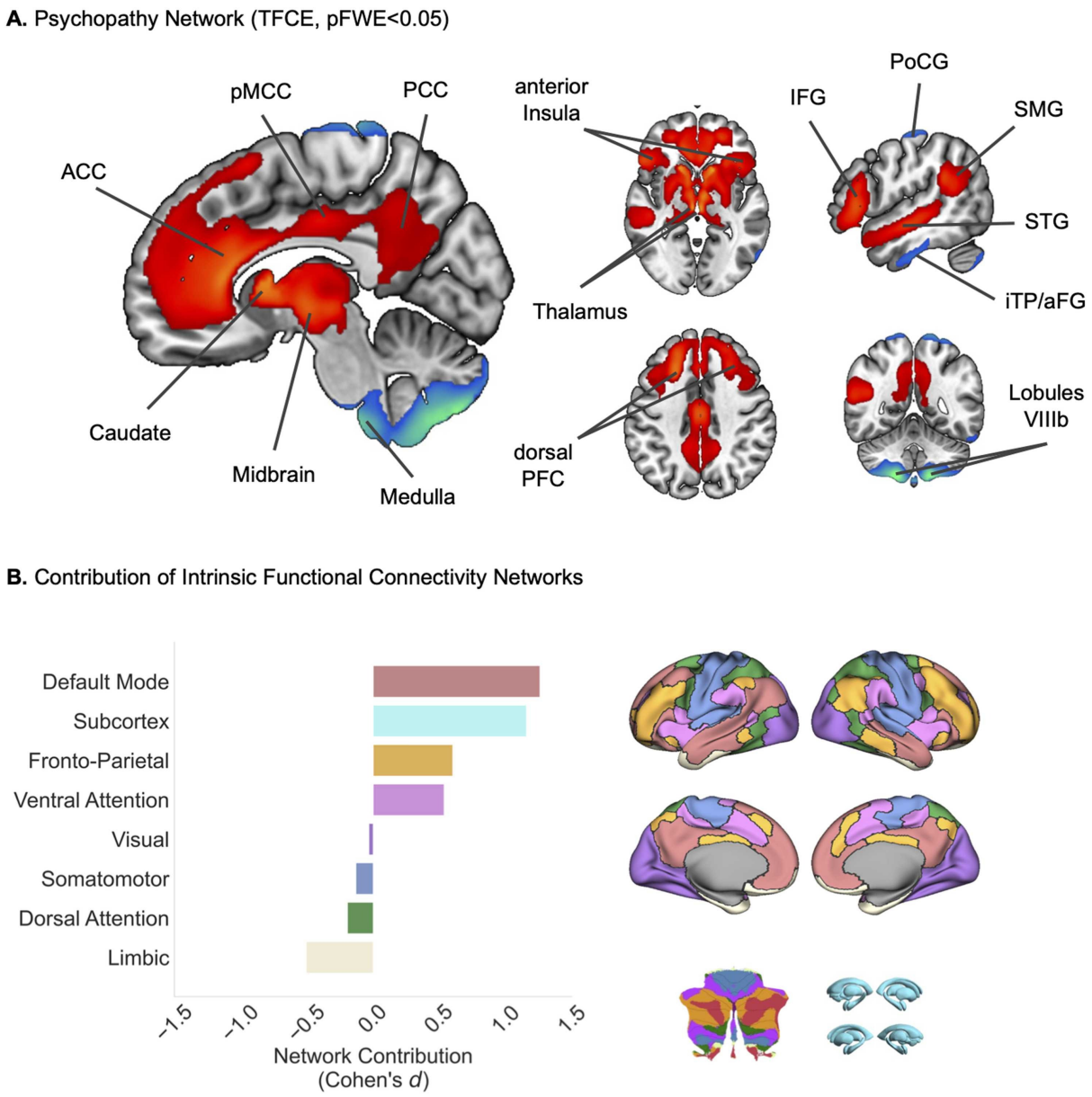

Figure 2.5: Neural Architecture of the Psychopathy Network. A. The Psychopathy Network (pFWE<0.05) included the following key hubs: the dorsal anterior cingulate cortex, midcingulate cortex, caudate nucleus, anterior insula, claustrum, dorsal/dorsolateral prefrontal cortex, thalamus/midbrain, inferior frontal gyrus, supramarginal gyrus, and anterior superior temporal gyrus. Peak coordinates across samples were negatively connected to lobules VIIIb, postcentral gyrus, inferior temporal pole, and medulla. B. Contribution of Intrinsic Functional Connectivity Networks highlighted the Default Mode Network (DMN) and Subcortex as core intrinsic networks characterizing the Psychopathy Network. The bar plot represents the effect size (Cohen's d) of each network's contribution. ACC = Anterior Cingulate Cortex; pMCC = posterior Midcingulate Cortex; PFC = Prefrontal Cortex; IFG = Inferior Frontal Gyrus; SMG = Supramarginal Gyrus; STG = Superior Temporal Gyrus[164].

differ widely in the seeds, parcellations, and statistical models, as summarized in a recent meta-analysis by Dugré and Potvin (2021)[166]. As a result, the underlying resting-state literature is methodologically heterogeneous, and the variations in ROI selection and analytical strategy are thought to contribute to the mixed pattern of reported abnormalities across studies. These issues have led to a growing interest in whole-brain frameworks that treat the entire connectome as a feature space, rather than restricting analyses to a small set of ROIs, and that explicitly test how well connectivity patterns can predict individual differences and generalize to new participants.

One of the proposed methods is Connectome-based Predictive Modelling (CPM)[167], a whole-brain machine learning framework designed to identify patterns of connectivity that predict individual-level behavioral traits. In particular, CPM and related whole-brain approaches have been successfully used to predict sustained attention[168], trait anxiety[169], as well as antipsychotic treatment response in first-episode psychosis[170], suicide risk in late-life depression[171], and compulsion severity in obsessive-compulsive disorder[172]. In the domain of psychopathy, a recent study employing CPM in the prediction of the Levenson Self-Report Psychopathy Scale (LSRP) in college students reported that regions, which negatively correlate with LSRP scores (e.g., anterior prefrontal cortex, anterior cingulate cortex, orbitofrontal cortex, and insula), successfully predicted both total and Factor 2 psychopathy scores, while Factor 1 scores was not robustly captured[173]. A clear benefit of CPM is that it quantifies how a pattern of connectivity across the entire brain can generalize to new individuals, rather than relying solely on group-level differences. Yet, despite these advances, the broader neuroimaging literature on psychopathy has several limitations that are directly relevant to the present thesis.

Limitations of Existing Literature

This section briefly outlines current limitations in neuroimaging and resting-state functional connectivity analysis in psychopathy research. Firstly, most structural and functional MRI studies of psychopathy have been conducted in forensic samples that are predominantly male[44], [119]. Research consistently notes that women with psychopathy or high psychopathic traits have been studied far less often, and that existing work on female offenders is limited[174]. A few recent resting-state fMRI studies have focused on incarcerated women[162] and high-risk adolescent girls[40]. Still, in the case of adolescents, these remain relatively modest in sample sizes (e.g., $n = 40$)[40], [162]. As a result, current neuroimaging models of psychopathy are still largely derived from male offender samples, and it is unclear to what extent these findings generalize to women or to individuals in the community.

Secondly, neuroimaging work on psychopathy has also been conducted mostly within Western criminal-justice and mental-health systems (e.g., North America and Western Europe), which mirrors the broader over-reliance of psychology and neuroscience studies on WEIRD samples[47]. This raises concerns about the cultural generalizability of findings and motivates further investigation of whether connectivity patterns linked to psychopathic traits will be expressed in the same way in different cultural contexts.

Finally, existing studies on psychopathy are often contrasting psychopathic individuals with non-psychopathic individuals, even though taxometric analyses of PCL-R and related measures indicate that psychopathy is better understood as a dimensional trait rather than a discrete category[58]. Treating psychopathy as a categorical diagnosis can obscure meaningful personality traits' variability within individuals in the general population, which limits both the theoretical precision and the clinical usefulness of brain-behavior findings.

To summarize, these limitations mean that there is still comparatively little known about how psychopathic traits are instantiated in the brains of females and males in the community, especially outside Western cultural contexts, and about how variation along the psychopathy continuum relates to intrinsic connectivity patterns. The present thesis, preregistered and conducted in line with current open-science recommendations (link), addresses these gaps by focusing on individual differences in psychopathic traits in mixed-sex community samples from distinct cultural settings, and by adopting a dimensional perspective on psychopathy by employing connectome-based predictive modelling. The idea of identifying neural correlates of psychopathy that can also map on individual differences in connectivity patterns of said correlates sets the stage for the present thesis.

2.4 Aims and Hypotheses

Based on established literature, I formulated the following research questions and predictions:

Research question 1. Can resting-state functional connectivity serve as a predictive marker of individual differences in psychopathy (Total score, Factor 1, Factor 2) within a Japanese community sample?

- **Hypothesis 1.1.** Whole-brain resting-state functional connectivity patterns will predict Total, Factor 1, and Factor 2 psychopathy scores in the Japanese community sample.

Research question 2. Which resting-state networks contribute most significantly to the prediction of psychopathy dimensions?

- **Hypothesis 2.1.** Higher psychopathy scores will be associated with stronger disconnection within the default mode network (i.e., medial prefrontal cortex, posterior cingulate), salience network (i.e., insula, anterior cingulate cortex), frontoparietal network (i.e., dorsolateral prefrontal cortex), and subcortical regions (i.e., amygdala, striatum).

Research question 3. Does a connectivity-based predictive model derived from the Japanese community sample generalize, without retraining, to predict the severity of psychopathic traits in an independent cohort from a different culture?

- **Hypothesis 3.1.** The model will generalize to the independent cohort, yielding significant, but likely attenuated, prediction of psychopathy scores relative to the original sample.

Exploratory analyses.

- Does weighted-sum CPM outperform unweighted CPM in cross-validated prediction of Total, Factor 1, and Factor 2?
- Does an NBS-derived subnetwork for feature selection yield more accurate cross-validated predictions of Total, Factor 1, and Factor 2 scores than conventional CPM-selected edges?
- Are there any sex differences in (a) the accuracy of CPM-based psychopathy predictions and (b) the specific connectivity patterns driving those predictions?

Due to the lack of prior research, these analyses are exploratory, and no a priori hypotheses were formulated.

3

Methods

3.1 Data Preparation

To investigate the relationship between brain function and psychopathic traits, and to test whether any brain-behavior associations would generalize across samples, I utilized two independently collected resting-state fMRI datasets. These comprised a cohort from Japan and a cohort from Germany. This section describes the demographic and acquisition details for each dataset, along with the standardized preprocessing pipeline applied to both cohorts to ensure data comparability.

3.1.1 Japanese dataset

The primary dataset is a cohort of structural and resting-state functional MRI scans collected from a Japanese community sample. This cohort comprises 97 healthy adult participants (right-handed, mean age = 26.9 $\pm$ 5.33, 52 females). One participant was excluded due to a missing fMRI scan, resulting in a total of 96 subjects analysed. Psychometric assessments and neuroimaging were conducted at Kyoto University, Japan. Psychopathic traits were measured via the Self-Reported Psychopathy Scale Fourth Edition (SRP-4) Short Form[175]. Participant's responses on the SRP-SF were aggregated to derive a total psychopathy score and four facet subscale scores: antisocial behaviour (ASB) (8 items, $\alpha = 0.63$), e.g., "I have assaulted a law enforcer or social worker"; callous affect (CA) (7 items, $\alpha = 0.67$), e.g., "I never feel guilty

when I hurt people"; interpersonal manipulation (IM)(7 items, $\alpha = 0.68$), e.g., "I like pushing people to their breaking point"; and erratic lifestyle (EL)(7 items, $\alpha = 0.82$), e.g., "I like having sex with people I barely know". For the present analyses, in line with established guidelines[68], I also computed a Factor 1 score by summing the CA and IM subscale responses (14 items, $\alpha = 0.85$), and a Factor 2 score by summing the ASB and EL subscale responses (15 items, $\alpha = 0.76$). All participants provided informed consent in accordance with the guidelines of the Ethics Committee at Kyoto University.

All magnetic resonance imaging was performed at Kyoto University on a Siemens 3T Verio scanner equipped with a 32-channel head coil. A high-resolution T1-weighted structural image was acquired using a Magnetization Prepared Rapid Acquisition Gradient Echo (MPRAGE) sequence. Acquisition parameters were: repetition time (TR) = 2500 ms, echo time (TE) = 2.18 ms, flip angle = 8°, field of view (FOV) = 256 mm, and voxel size = 0.8*x*0.8*x*0.8 mm, yielding 224 sagittal slices. The total scan duration was 5 minutes and 22 seconds. fMRI images were acquired using an echo-planar imaging (EPI) sequence covering the entire brain. Acquisition parameters were: TR = 1300 ms, TE = 40 ms, flip angle = 66°, FOV = 24 cm, and voxel size = 2.5*x*2.5*x*2.5 mm. A total of 60 axial slices were acquired. The functional scan lasted 10 minutes.

3.1.2 German dataset

The second dataset was sourced from MPI-Leipzig Mind-Brain-Body open-access database[176]. The initial available cohort included 107 healthy participants (age range = 20–80; 68 females). However, to ensure demographic comparability with the Japanese dataset, this sample was later restricted to match the age range of the primary cohort, resulting in a total of 87 participants (age range = 20–35; 48 females). Psychometric assessments and neuroimaging were conducted at the Max Planck Institute for Human Cognitive Neurology at the University of Leipzig, Germany, as part of the MPI-Leipzig Mind-Brain-Body functional connectome phenotyping project[177]. Participants completed the Short Dark Triad (SD3) in addition to other personality measures. In the present analyses, the psychopathy SD3 subscale (e.g., "It's true that I can be mean to others") was used as the target variable for testing hypotheses. All participants provided written informed consent, and the study was approved by the ethics committee at the medical faculty of the University of Leipzig.

High-resolution T1-weighted structural images were acquired on a 3T Siemens Magnetom Verio scanner using a 3D Magnetization-Prepared 2 Rapid Acquisition Gradient Echos (MP2RAGE) sequence. Acquisition parameters were: TR = 5000 ms, TE = 2.92 ms, flip angles = 4° and

5°, FOV = 256*x*240*x*176 mm, and voxel size = 1.0*x*1.0*x*1.0 mm, resulting in a single 3D volume with 176 sagittal slices. Resting-state fMRI images were acquired using a T2*-weighted gradient-echo EPI sequence. Acquisition parameters: TR = 1400 ms, TE = 39.4 ms, flip angle = 69, FOV = 202*x*202 mm^2, voxel size = 2.3*x*2.3*x*2.3 mm, and 64 axial slices. Each run consisted of 657 volumes and lasted 15 minutes and 30 seconds.

3.1.3 Data preprocessing (CONN toolbox)

All rs-fMRI data from both cohorts were preprocessed using the CONN (22.v2407) functional connectivity toolbox[178]. The default preprocessing pipeline was employed. Specifically, functional and anatomical data were preprocessed using a modular preprocessing pipeline[179] including realignment with correction of susceptibility distortion interactions, slice timing correction, outlier detection, direct segmentation and MNI-space normalization, and smoothing. The functional data were realigned using SPM realign and unwarp procedure[180], where all scans were coregistered to a reference image (first scan) using a least squares approach and a 6 parameter (rigid body) transformation[181], and resampled using b-spline interpolation to correct for motion and magnetic susceptibility interactions. Temporal misalignment between different slices of the functional data (acquired in interleaved Siemens order) was corrected following SPM slice-timing correction (STC) procedure[182], [183], using sinc temporal interpolation to resample each slice BOLD timeseries to a common mid-acquisition time. Potential outlier scans were identified using ART[184] as acquisitions with framewise displacement above 0.9 mm or global BOLD signal changes above 5 standard deviations[185], [186], and a reference BOLD image was computed for each subject by averaging all scans excluding outliers. Functional and anatomical data were normalized into standard MNI space, segmented into grey matter, white matter, and CSF tissue classes, and resampled to 2 mm isotropic voxels following a direct normalization procedure[186], [187] using SPM unified segmentation and normalization algorithm[188], [189] with the default IXI-549 tissue probability map template. Last, functional data were smoothed using spatial convolution with a Gaussian kernel of 6 mm full width half maximum (FWHM)[190].

3.1.4 Connectome Construction

Following data preprocessing, brain activity was first summarized into a set of functionally homogeneous regions (parcels) that served as nodes in the functional connectome. Cortical parcels were defined using the 400-region Schaefer atlas[191], supplemented by a standard set

of subcortical[192] and cerebellar[193] ROIs, resulting in a total of $P = 421$ distinct nodes.

To map each individual's brain organization at rest, functional connectivity was measured to reflect the co-activation between pairs of regions over time. First, the mean pre-processed BOLD time series was extracted from each ROI for every subject. These time courses were band-pass filtered between 0.008 and 0.09 Hz. Functional connectivity was defined as a measure of strength and direction of a linear relationship between two time series. This was achieved by computing the Pearson correlation coefficient (r) between every pair of ROI signals. Mathematically, Pearson correlation between two time series $x(t)$ and $y(t)$ is:

$$r_{XY} = \frac{\sum_{t=1}^{T}(x_t - \bar{x})(y_t - \bar{y})}{\sqrt{\sum_{t=1}^{T}(x_t - \bar{x})^2}\sqrt{\sum_{t=1}^{T}(y_t - \bar{y})^2}} \tag{3.1}$$

where x_t and y_t denote the BOLD signal at time point t in each region, $\bar{x}$ and $\bar{y}$ are the mean signals across time points, and T is the number of time points in the time series. Applying pairwise Pearson correlation produced a $P \times P$ correlation matrix for each participant, where each entry represents the strength of a functional connection between two nodes. Finally, all correlation values were transformed using Fisher's z-transformation to stabilize variance for subsequent analyses:

$$z_{XY} = \operatorname{arctanh}(r_{XY}) = \frac{1}{2}\ln\left(\frac{1 + r_{XY}}{1 - r_{XY}}\right) \tag{3.2}$$

For sufficiently large T, the transformed values z_{XY} are approximately normally distributed with variance $\approx 1/(T - 3)$, which makes them more suitable for use in linear models. The resulting connectome provided a unique representation of each individual's whole-brain functional organization, serving as the primary data for the predictive modelling described in the next section.

3.2 Connectome-Based Predictive Modelling

Connectome-based predictive modelling is a data-driven framework that uses whole-brain functional connectivity patterns to predict individual differences in behavior or clinical traits. This approach typically involves several key stages: (1) feature selection to identify trait-relevant connections, (2) feature summarization to create a single 'network strength' score per participant, (3) model building to relate network strength to the behavioral trait, and (4) a rigorous

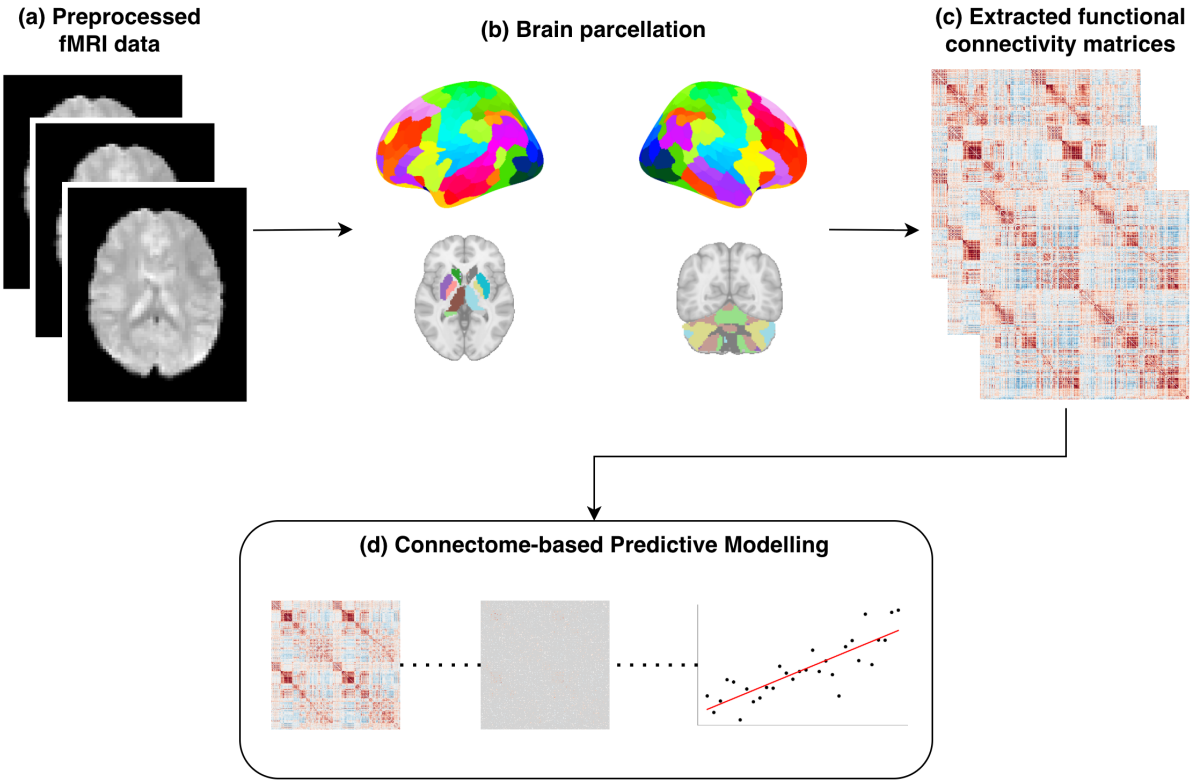

Figure 3.1: Overview of the analytical pipeline. (a) Preprocessed resting-state fMRI data were obtained for each participant; (b) data were parcellated using a standard cortical and subcortical atlas; (c) subject-specific functional connectivity matrices were extracted; (d) the matrices were used as an input to connectome-based predictive modeling to test whether whole-brain connectivity predicts individual differences in psychopathic traits.

assessment of the model's predictive significance, often using permutation testing[167].

After data preprocessing and connectome construction, the CPM was applied to achieve three primary objectives. First, to test whether individual differences in whole-brain functional connectivity could successfully predict psychopathic traits (Total, Factor 1, and Factor 2 scores). Second, to identify the specific neural circuits driving this prediction. And third, to assess whether the predictive model generalizes to a dataset with a different cultural background (see Hypotheses 2.4).

Given the established success to predict a range of individual differences from whole-brain FC[194], [195], [196], [197], [198], CPM was selected as the primary tool to address the previously outlined hypotheses: (H1.1) whole-brain rsFC patterns will predict total, Factor 1, and Factor 2 psychopathy scores in the Japanese community sample, and (H3.1) a model derived in this sample will generalize, without retraining, to predict psychopathic traits in an independent German cohort.

Importantly, CPM yields not only prediction scores but also produces a set of predictive edges (functional connections whose strength reliably relates to the target trait). These edge sets can be projected onto canonical resting-state networks, allowing us to characterize which large-scale

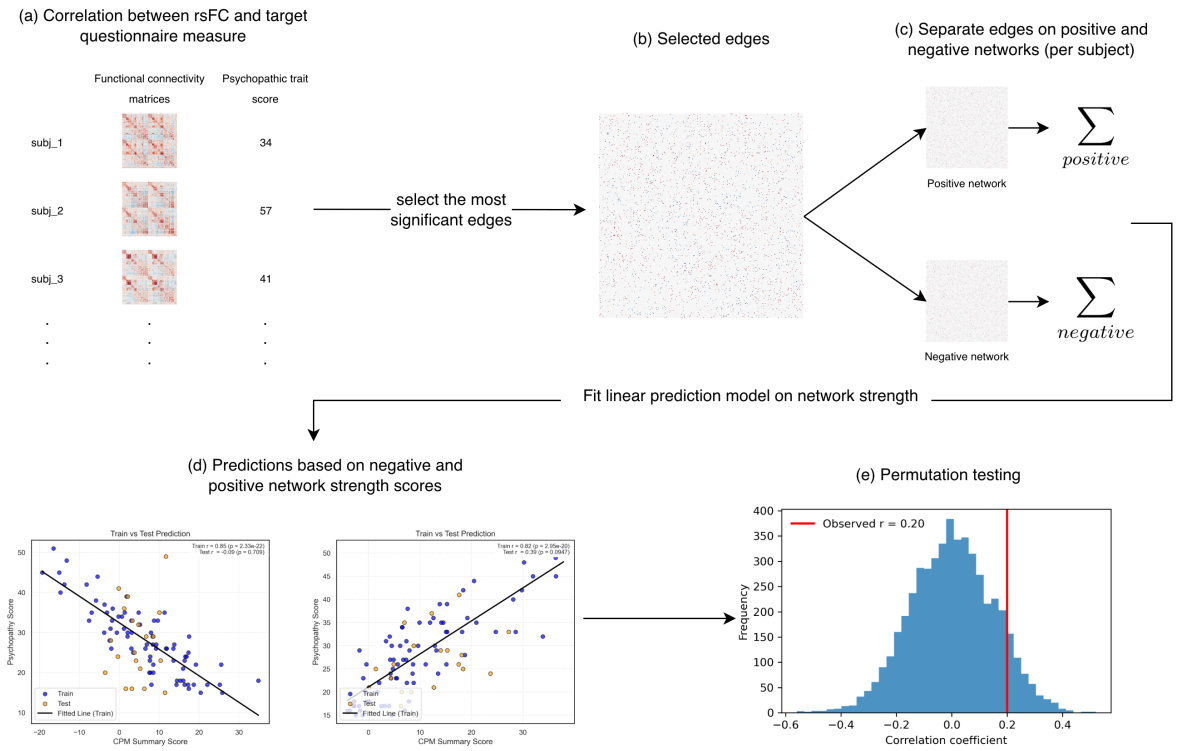

Figure 3.2: Overview of the connectome-based predictive modeling (CPM) pipeline. Schematic overview of the connectome-based predictive modeling (CPM) pipeline used in this study. (a) For each participant, whole-brain resting-state functional connectivity (rsFC) matrices are correlated with individual psychopathic trait scores at the edge level. (b) Edges that exceed a predefined significance threshold are selected. (c) Significant edges are divided into positive and negative networks, and for each subject network strength scores are computed by summing edge weights within each network. (d) Positive and negative network strength scores are entered into a linear model to predict psychopathy scores in the training set and generate out-of-sample predictions in the test set. (e) Model performance is assessed with permutation testing by shuffling psychopathy scores to build a null distribution of prediction coefficients and comparing it with the observed correlation.

networks contribute most strongly to the predictions. Hence, CPM-derived edges allow me to address H2.1, which is whether higher psychopathy scores will be associated with stronger disconnection within the default mode, salience, frontoparietal networks, and subcortical regions.

3.2.1 Baseline CPM implementation

To test Hypotheses 1.1 and 3.1, subject-wise resting-state functional connectivity (rsFC) matrices as predictors and psychopathy scores as target variables were used. For each participant $i = 1, \dots, N$, rsFC was summarized as a symmetric matrix $C_i \in \mathbb{R}^{P \times P}$, where $P = 421$ is the number of cortical, subcortical, and cerebellum parcels. Each entry $c_i(p, q)$ is the Fisher-z transformed Pearson correlation between the preprocessed BOLD time series of parcels p and q. Since connectivity matrices are symmetrical, the duplicate values are removed by vectorizing the upper triangle of each matrix C_i (excluding the diagonal) into a connectivity vector $\mathbf{x}_i \in \mathbb{R}^E$, where $E = P(P-1)/2$ is the number of resulting edges. Stacking these vectors yielded an $N \times E$ feature matrix

$$\mathbf{X} = \begin{bmatrix} \mathbf{x}_1^\top \\ \mathbf{x}_2^\top \\ \vdots \\ \mathbf{x}_N^\top \end{bmatrix}.$$

$\mathbf{x}_{\cdot e}$ denotes the N-dimensional column vector containing the connectivity of edge e across all subjects:

$$\mathbf{x}_{\cdot e} = (x_{1e}, x_{2e}, \dots, x_{Ne})^\top, \quad e = 1, \dots, E.$$

Psychopathic traits were represented by a behavioral vector $\mathbf{y} = (y_1, \dots, y_N)^\top$ where y_i denotes the score of subject i on the relevant dimension (Total, Factor 1, or Factor 2; additional facet scores were considered in exploratory analyses).

To identify edges that are informative for predicting psychopathic traits (H1.1, H3.1), CPM performs feature selection separately within each training fold. For each edge $e = 1, \dots, E$, the Pearson correlation is computed between its connectivity strength across subjects $\mathbf{x}_{\cdot e}$, and the corresponding psychopathy scores y: $r_e = \mathrm{corr}(x_{\cdot e}, y)$. This results into a set of edge-wise correlations $\{r_e\}_{e=1}^{E}$ and associated p-values computed within the training subjects of that fold. Commonly, edges are then thresholded according to a fixed significance value (e.g., two-tailed $p < 0.01$) to define a set of edges associated with the target score y. However, in this study I did not fix a single threshold. Instead, a set of candidate thresholds was proposed, specifically $\mathcal{A} = \{0.01, 0.025, 0.05\}$, and the feature selection and model-building steps were repeated for

each $\alpha \in \mathscr{A}$.

Then, positive and negative networks were defined by looking at r_e. Positive edges are those for which higher connectivity is associated with higher psychopathy scores, whereas negative edges show the opposite pattern. Formally, we define the positive and negative edges as

$$E^+ = \{e \in \{1, \dots, E\} : r_e > 0 \wedge p_e < \alpha\}, \qquad E^- = \{e \in \{1, \dots, E\} : r_e < 0 \wedge p_e < \alpha\},$$

where α denotes the chosen threshold. Feature selection is recomputed independently in each cross-validation fold using only the training data so that the information from test subjects does not leak into the model-building stage. The resulting edge sets E^+ and E^- form the basis for the computation of network strength scores. The selected predictive edges also provide the building blocks for later analysis of psychopathy-related connectivity patterns (H2.1).

To transform the high-dimensional connectivity into low-dimensional predictors, CPM aggregates the selected edges into summary scores, known as "network strength" scores. For each cross-validation split, we compute positive and negative network strengths for every subject i by summing the connectivity values of the edges in the corresponding sets E^+ and E^-:

$$S_i^+ = \sum_{e \in E^+} x_{ie}, \qquad S_i^- = \sum_{e \in E^-} x_{ie},$$

where x_{ie} denotes the connectivity strength of edge e for subject i. The resulting scalars S_i^+ and S_i^- quantify, respectively, the overall strength of edges where higher connectivity is associated with higher psychopathy scores and those where lower connectivity is associated with higher scores. These network strengths are the standard CPM feature summaries and have been shown to provide robust and interpretable predictors that retain information from connectivity patterns while greatly reducing dimensionality.

To test Hypothesis 1.1 that whole-brain rsFC patterns predict Total, Factor 1, and Factor 2 psychopathy scores within the Japanese community sample, a nested cross-validation (CV) was implemented for the CPM. Specifically, $K_{\text{outer}} = 5$ outer folds, and within each outer training set, $K_{\text{inner}} = 5$ inner folds for parameter selection and edge stability assessment were employed. The outer CV loop intends to provide an unbiased estimate of the out-of-sample predictive performance, while the inner loop is used to select the best feature-selection threshold α in $\mathscr{A} = \{0.01, 0.025, 0.05\}$ and to quantify the stability of predictive edges. Notably, to provide a better validated metrics, the outer CV was repeated 50 times.

For each outer training set the CPM was performed within the inner folds as follows:

1. In each inner training fold, feature selection was executed for each candidate threshold $\alpha \in \mathcal{A}$, obtaining edge sets $E^{+}(\alpha)$ and $E^{-}(\alpha)$, and then the corresponding network strengths $S^{+}(\alpha)$ and $S^{-}(\alpha)$ were computed.

2. For each alpha, a linear regression model was fitted on the inner fold train set

$$y_i = \beta_0 + \beta_1 S_i^{+}(\alpha) + \beta_2 S_i^{-}(\alpha) + \gamma^{\top}\mathbf{z}_i + \varepsilon_i,$$

where y_i denotes the psychopathy score of subject i, $\mathbf{z}_i$ - the covariates (when included), $beta_0$ the intercept, $beta_1$ and $beta_2$ the coefficients for the positive and negative CPM networks, and γ the coefficients for covariates.

3. Using the fitted coefficients, predictions were generated in the inner validation folds, and the Spearman correlation was computed between predicted and observed scores for each alpha:

$$\rho^{(\text{inner})} = \text{corr}_{\text{Spearman}}(\hat{\mathbf{y}}, \mathbf{y}).$$

The threshold alpha* that yielded the best average inner-loop performance was selected for that outer training set:

$$\alpha^{*} = \arg\max_{\alpha \in \mathcal{A}} \bar{\rho}(\alpha).$$

4. In parallel, for each edge the algorithm recorded how often it was selected into the positive and negative networks across the inner folds with the optimal threshold alpha*.

$$\pi_e^{+},\ \pi_e^{-}, \quad \text{where} \quad \pi_e^{+/-} \in [0, 1]$$

is the proportion of inner folds in which edge e appeared in $E^{+/-}(\alpha^{*})$.

5. Then, the stability threshold of 0.6 was applied to define the final sets of stable positive and negative edges:

$$E^{+}_{\text{stable}} = \{e : \pi_e^{+} > 0.6\}, \qquad E^{-}_{\text{stable}} = \{e : \pi_e^{-} > 0.6\}.$$

In this way, only edges that were consistently selected across inner folds were carried forward to the outer loop.

For each outer fold, where the test subjects were held out completely, the CPM model was

fitted on the entire outer training set using the stable edge sets derived from the corresponding inner loop:

1. Using E^{-}_{stable} and E^{+}_{stable}, the algorithm computed positive and negative network strengths for all subjects in the outer training and test sets (S_i^+, S_i^-).

2. Next, the CPM regression model was fitted on the outer training subjects

$$y_i = \beta_0 + \beta_1 S_i^+ + \beta_2 S_i^- + \gamma^\top \mathbf{z}_i + \varepsilon_i,$$

   Where y_i denotes the psychopathy score of subject i, $\mathbf{z}_i$ the covariates (if included), $beta_0$ the intercept, $beta_1$ and $beta_2$ the coefficients for the positive and negative CPM networks, γ the covariate coefficients, and ε_i the error term.

3. In addition to the model outlined above, separate linear regression models were used for negative or positive network summary scores, thus providing separate linear models for each network type.

4. To investigate the effect of covariates, a model using only covariates to predict scores was implemented.

5. The fitted coefficients ($beta_0, beta_1, beta_2, \gamma$) were then applied to the network strengths of the outer test subjects to obtain out-of-sample predictions $\hat{y}_i^{(t)}$.

Additionally, a confound-corrected[199] variant of the model was implemented in which the effects of covariates were regressed out of the CPM network-strength features before prediction. For each network (positive, negative, both) and each subject i, C_i denotes the corresponding network-strength vector, and $\mathbf{z}_i$ the covariate vector. Within the outer training set, a linear regression model was fitted:

$$C_i = a_0 + A^\top \mathbf{z}_i + \eta_i.$$

It resulted in covariate-adjusted CPM features as the residuals:

$$R_i = C_i - (a_0 + A^\top \mathbf{z}_i)$$

where $\hat{a}_0$ and $\hat{A}$ are the regression coefficients estimated from the outer training data. The same fitted model was then used to compute residualized features R_i for the outer test subjects.

Using these predictors, four related linear models were estimated in each outer fold: (1)

a connectome-only model using C_i as predictors; (2) a covariates-only model using z_i; (3) a residuals-only model using the confound-regressed features R_i; and (4) a full model that combined CPM features and covariates. Comparing performance across these models allowed me to quantify how much variance in psychopathy scores was explained by covariates alone, by CPM features alone, and by CPM features after removal of linear covariate effects, while still basing all performance estimates on outer-fold predictions for unseen subjects.

To test Hypothesis 3.1, the CPM model was trained on the Japanese community sample. The German cohort was then used as an external out-of-sample test set to examine whether the connectivity-psychopathy associations learned in the Japanese sample generalized to a different cultural context.

3.2.2 Weighted CPM (exploratory)

This subsection addresses research question 4, namely whether a weighted-sum implementation of CPM improves prediction relative to the standard unweighted network-strength model. As established earlier, in the baseline CPM, all edges within the positive and negative networks contribute equally to the network-strength scores (sum of selected edges). This implicitly assumes that edges with weak and strong brain-behavior associations are equally informative. However, in weighted CPM, we instead assign larger weights to edges whose connectivity shows stronger associations with the psychopathy scores in the training data. In this way, the network-strength scores are more heavily driven by edges that consistently covary with the outcome, while edges with weaker or more unstable associations contribute proportionally less.

For each fold, network (positive/negative) and target score, the algorithm took the correlation coefficient r_e between edge e and the behavioral score (estimated in training data, see section 3.2.1) and computed their absolute values $|r_e|$ within the set of selected edges. Edges were then ranked in descending order of $|r_e|$ with ranks $R_e = 1, 2, 3, \ldots$. The weight was defined as an inverse of this rank: $\tilde{w}_e = 1/R_e$ which were normalized within each network so that they sum to 1.

$$w_e = \frac{\tilde{w}_e}{\sum_{j \in E^+} \tilde{w}_j} \text{ for } e \in E^+, \qquad w_e = \frac{\tilde{w}_e}{\sum_{j \in E^-} \tilde{w}_j} \text{ for } e \in E^-.$$

This allowed for the largest $|r_e|$ edge to receive the largest weight. Weighted positive and negative network strengths for subject i were then computed as

$$S^+_{i,w} = \sum_{e \in E^+} w_e x_{ie}, \qquad S^-_{i,w} = \sum_{e \in E^-} w_e x_{ie},$$

where x_{ie} is the connectivity value of edge e for subject i. These weighted scores replace the unweighted sums used in the baseline CPM but are otherwise entered into the same linear regression framework with nested cross-validation described in Section 3.2.1.

3.2.3 Network-Based Statistic+CPM (exploratory)

This subsection addresses Research Question 5, specifically whether subnetworks derived with a network-based statistic (NBS) approach provide different or improved predictions compared with conventional CPM edge selection. The NBS was originally proposed as a way to detect clusters of connected edges that are associated with a variable of interest, while controlling family-wise error at the component level rather than at individual edges[200]. In standard NBS, one first applies a primary edge-wise threshold to a connectivity statistic, then identifies connected components (subnetworks) of suprathreshold edges, and finally uses permutation testing to assess whether the size of each component is unlikely under null. This makes NBS particularly suited to finding spatially extended topologically coherent connectivity patterns. Recent developments in the field of connectome-based machine learning introduced an NBS-Predict algorithm that extends the idea by combining NBS components with machine learning models which are used to predict behavior. This approach is thought to improve performance and interpretability, since features come as connected subnetworks that explicitly include network topology information into the modelling process[201].

The proposed NBS+CPM approach follows the same framework as baseline CPM, but instead of univariate feature selection, it restricts the selected edges to those that belong to coherent subnetworks. The rest of the CPM pipeline (network-strength computation, linear models, nested cross-validation) is left unchanged.

Within each training set of the nested cross-validation (inner and outer folds), NBS+CPM defines positive and negative subnetworks in the following steps:

1. For each edge e, a Pearson correlation r_e between connectivity and scores was computed and transformed into a t-statistic

$$t_e = r_e \sqrt{\frac{\mathrm{df}}{1 - r_e^2}},$$

with $\mathrm{df} = N - 2$, where N is the number of subjects in that training set.

2. Next, a two-tales primary threshold $\alpha = 0.05$ was applied to these statistics, keeping edges with $|t_e| > t_{\mathrm{crit}}$ corresponding to $p < 0.05$. Suprathreshold edges with $t_e > 0$ form

the positive graph, and those with $t_e < 0$ form the negative graph, where parcels represent nodes and suprathreshold connections as edges.

3. The suprathreshold graphs obtained can contain many small "whiskers" (single edges or chains of 2-3 edges) that are weakly embedded in the overall network. To focus on more cohesive subnetworks, two graph-theoretic operations were applied:

   (a) K-score pruning, which restricts each graph to its k-core with $k = 2$. A k-core is the largest subgraph in which every node has degree at least k. Operationally, nodes with fewer than two suprathreshold connections are iteratively removed until all remaining nodes satisfy $\deg(v) \geq 2$ for all v

   (b) Bridge pruning, which removes edges that act like bridges - edges whose removal would disconnect the graph into two components. Therefore, all such bridge edges were removed using a standard depth-first search (DFS) algorithm. The resulting subnetworks come out as more internally cohesive and less dependent on single "critical" links.

4. Lastly, the connected components were identified using DFS applied to the pruned graph. For each positive and negative sign, the largest connected component by edge count was selected (denoted E^{+}_{NBS} and E^{-}_{NBS}). The others were discarded.

Across inner folds, we sought subnetworks that are reproducible rather than constrained to a single split. For each psychopathic score and sign ($s \in \{+, -\}$), I therefore performed component-aware stability based on overlaps of edge sets across inner folds. Let F be the number of inner folds. For each fold $f = 1, \ldots, F$ and sign s, denote by $E_f^{(s)} \subseteq \{1, \ldots, E\}$ the edge set of the NBS subnetwork obtained in that fold, where E is the total number of possible edges. Similarity between subnetworks from folds f and g was quantified using Jaccard index

$$J(E_f^{(s)}, E_g^{(s)}) = \frac{|E_f^{(s)} \cap E_g^{(s)}|}{|E_f^{(s)} \cup E_g^{(s)}|}.$$

In the current process, two fold-specific subnetworks were considered to belong to the same component if $J(E_f^{(s)}, E_g^{(s)}) \geq 0.2$. At least 60% of folds have to form a set of clusters with Jaccard similarity ≥ 0.2. Next, edge-wise stability across inner folds was computed. Edges were retained if their stability index is ≥ 0.6.

After enforcing that this consensus again forms a single largest connected component, we ob-

tain stable NBS subnetworks $E^{+}_{\text{NBS,stable}}, E^{-}_{\text{NBS,stable}}$. In each outer training set, these subnetworks are summarized into network strength scores for subject i,

$$S^{+}_{i,\text{NBS}} = \sum_{e \in E^{+}_{\text{NBS,stable}}} x_{ie}, \qquad S^{-}_{i,\text{NBS}} = \sum_{e \in E^{-}_{\text{NBS,stable}}} x_{ie}$$

and these replace the baseline CPM strengths in the same family of connectome-only, residuals-only, and full linear models implemented. Prediction and nested cross-validation proceed exactly as described in Section 3.2.1. To address research question 5, I then compare NBS+CPM and standard CPM, examining the models' predictive performance.

3.3 Evaluation metrics

This section defines how I quantify "successful prediction", how I test Hypothesis 1.1 (prediction within the Japanese sample) and Hypothesis 3.1 (generalization in the German sample), and how I interpret exploratory model variants (weighted CPM and NBS+CPM; research questions 4-5).

For each model, psychopathy score and dataset, predictive performance was evaluated using out-of-sample predictions from the outer folds of the nested cross-validation. Let y_i denote the observed score for subject i and $\hat{y}_i$ the corresponding predicted score. Across all subjects per fold, the metrics computed were:

1. Pearson correlation between predicted and observed scores,

$$r = \text{corr}(\hat{y}, y),$$

   which is the conventional primary performance metric in CPM.

2. Mean absolute error (MAE)

$$\text{MAE} = \frac{1}{N} \sum_{i=1}^{N} |\hat{y}_i - y_i|,$$

   which quantifies the absolute deviation of predictions from the observed scores in the target variable's original units.

3. Coefficient of determination (R^2)

$$R^2 = 1 - \frac{\sum_{i=1}^{N} (y_i - \hat{y}_i)^2}{\sum_{i=1}^{N} (y_i - \bar{y})^2}$$

representing goodness-of-fit measure for linear regression models, where $\hat{y}$ is the mean observed score across subjects.

All metrics were computed on test data only; no subject contributed both to the training and test sets for a given outer-fold prediction. When models were repeated multiple times, their performance was summarized as the mean and standard deviation of the metrics.

3.3.1 Permutation testing

To test whether predictive performance exceeded what would be expected by chance, permutation testing was employed at the level of the CPM pipeline. For each psychopathy score and model configuration, a null distribution of performance was constructed by repeatedly shuffling the correspondence between functional connectivity and outcome scores and rerunning the full analysis:

1. For a given dataset and outcome variable, $B = 5000$ permutations were generated. In permutation b, the psychopathic scores across subjects were randomly permuted, obtaining a vector $y^{(b)}$ that preserves the marginal distribution of scores, but removes any true association with the connectomes.

2. For each permuted outcome $y^{(b)}$, the entire CPM pipeline was rerun, including nested cross-validation, feature selection, network strength computation, model fitting, and out-of-sample prediction, exactly as for the original data. This yielded permuted performance metrics for each permutation, such as correlation scores or error metrics, which we denote $m^{(b)}$.

   The collection of permutation metrics defines the null distribution of predictive performance under the hypothesis that rsFC and psychopathic scores are unrelated. For the observed (non-permuted) data, the actual performance is computed.

3. To assess the significance of the models' performance, for each metric and model, the algorithm compared the observed performance m_{obs} (from the non-permuted data) to the set of permuted values $\{m^{(b)}\}_{b=1}^{B}$.

   (a) For score metrics, where higher values indicate better prediction, the permutation p-value was defined as

$$p_{\text{perm}} = \frac{\#(b : m^{(b)} \geq m_{\text{obs}})}{B + 1}$$

indicating a fraction of permutation runs in which a model trained on permuted outcomes achieved a higher score than the model trained on the true outcomes.

(b) For error metrics, where lower values indicate better prediction, the inequality was reversed:

$$p_{\text{perm}} = \frac{\#(b : m^{(b)} < m_{\text{obs}})}{B + 1}$$

corresponding to the fraction of permutation runs in which a model trained on permuted outcomes achieved a smaller error than observed.

In this way, p_{perm} quantifies how often a model trained on shuffled labels outperformed the model trained on true labels. Hypothesis 1.1 (prediction within the Japanese sample) and Hypothesis 3.1 (prediction within the German sample) were considered supported only when permutation p-values for the baseline model were below the significance threshold ($p < 0.05$).

In addition, for the stability analyses, null distributions were also constructed for edge stability across permutations. For each edge, the proportion of permutation runs was computed in which its stability was at least as high as in the non-permuted data, yielding an edge-wise stability p-value.

4

Results

To test the central hypotheses (Section 2.4) regarding the neural underpinnings of psychopathy, I first implemented a connectome-based predictive modeling approach. More precisely, I examined whether resting-state functional connectivity could predict the total psychopathic score, as well as Factor 1 and Factor 2, in a Japanese community sample. Second, in a set of exploratory analyses, I evaluated (a) alternative model implementations (weighted CPM and NBS + CPM), (b) potential sex differences, and (c) cross-dataset generalization to an independent German cohort. Finally, I also fitted CPM models for the four SRP-SF facet scores to explore more fine-grained relationships between functional connectivity and psychopathy traits.

4.1 RQ1: Prediction of Psychopathic Traits from rsFC (H1.1.)

During model training, CPM showed an excellent fit to the data. Across cross-validation folds, the average Pearson correlation, which quantifies the linear association between predicted and observed values, in the training sets was high (mean $r \approx 0.85$ for Total, Factor 1 and Factor 2).

However, contrary to my main hypothesis (Section 2.4), this fit did not generalize to the test data. CPM models trained on whole-brain functional connectivity did not yield significant out-of-sample predictions for total, Factor 1, or Factor 2 scores. As detailed in Table 4.1, the average test-set Pearson's r across all cross-validation folds was near zero.

Permutation tests supported the null result by generating a null distribution of test-set correla-

Table 4.1: Baseline CPM performance (mean [sd] across CV repeats) with permutation p-values.

			MAE		Pearson r	
Target	**Model**	**Network**	**mean [sd]**	p	**mean [sd]**	p
Total	connectome	positive	12.66 [1.64]	0.553	0.09 [0.20]	0.234
		negative	12.64 [1.75]	0.525	-0.00 [0.25]	0.522
		both	12.46 [1.64]	0.645	0.05 [0.23]	0.365
	residuals	positive	12.69 [1.61]	0.519	0.09 [0.20]	0.227
		negative	12.79 [1.81]	0.561	-0.02 [0.24]	0.560
		both	12.56 [1.72]	0.638	0.04 [0.23]	0.368
Factor 1	connectome	positive	8.00 [1.07]	0.681	0.06 [0.20]	0.307
		negative	7.99 [1.06]	0.644	-0.01 [0.22]	0.528
		both	7.87 [0.99]	0.799	0.03 [0.20]	0.396
	residuals	positive	7.94 [1.04]	0.572	0.09 [0.20]	0.224
		negative	7.99 [1.09]	0.602	0.00 [0.22]	0.483
		both	7.84 [1.04]	0.692	0.06 [0.20]	0.313
Factor 2	connectome	positive	5.19 [0.82]	0.192	0.11 [0.23]	0.169
		negative	5.39 [0.83]	0.424	-0.00 [0.27]	0.510
		both	5.23 [0.80]	0.403	0.06 [0.27]	0.321
	residuals	positive	5.38 [0.81]	0.380	0.06 [0.22]	0.303
		negative	5.63 [0.83]	0.691	-0.11 [0.23]	0.836
		both	5.47 [0.81]	0.718	-0.01 [0.24]	0.524

tions and calculating the proportion of these null correlations that are at least as large as the one observed with the true data. All permutation p-values were well above the significance threshold ($(p > 0.2)$), meaning that the observed performance is not different from the one generated by chance. Furthermore, the mean absolute error (MAE) values were comparable to a mean-prediction baseline (e.g., Total score baseline $\approx$ 11.4; Factor 1 $\approx$ 7.0; Factor 2 $\approx$ 4.9). This shows that models did not outperform trivial predictions of the sample mean.

Figure 4.1 illustrates a representative cross-validation repeat, comprising subsequent 5 folds in the cross-validation procedure, where test predictions cluster around the sample mean, consistent with negligible predictive variance and a lack of linear relationship.

4.2 RQ2: Contributing Resting-state Networks (H2.1.)

I originally sought to examine whether any predictive effects would be driven by connections within particular intrinsic resting-state networks (default mode, salience, frontoparietal control). However, this analysis was contingent on a significant finding for RQ1. Since the target baseline CPM models for psychopathy Total and Factor scores did not achieve significant out-of-sample performance (see Section 4.1), Hypothesis 2.1 could not be tested and no network-level conclu-

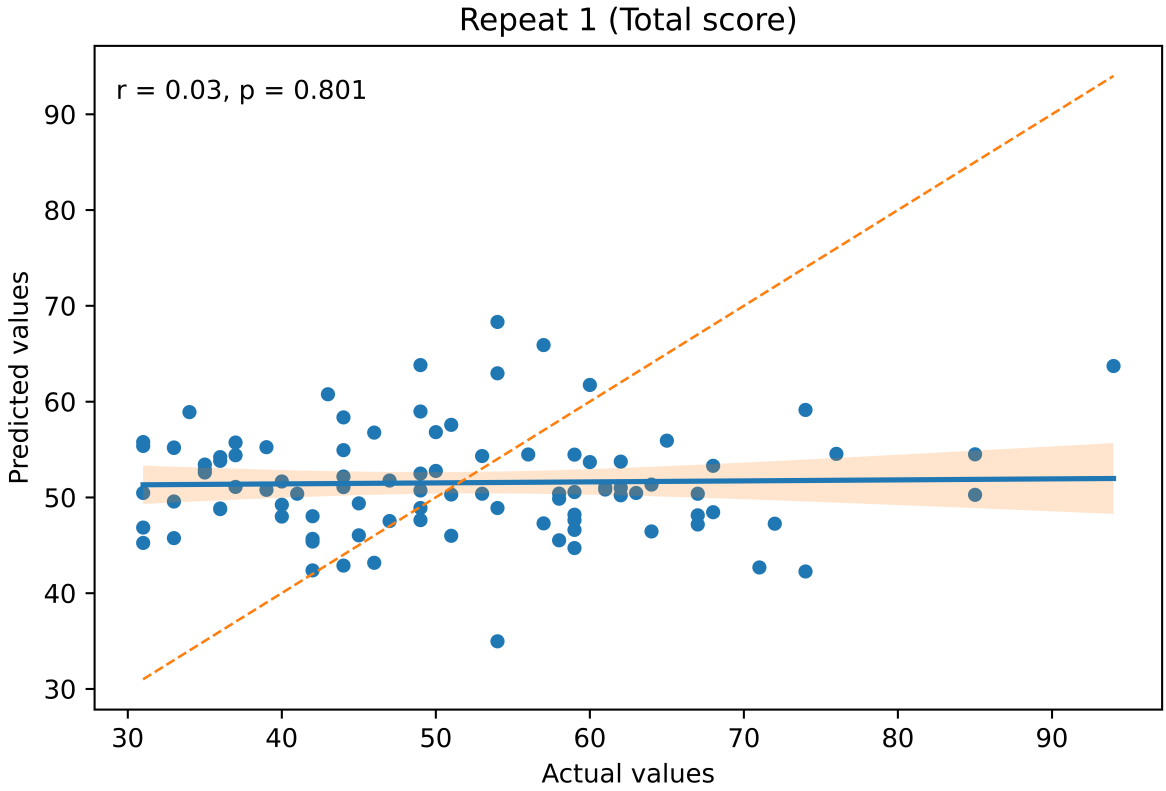

Figure 4.1: Example test set scatter plot from a single cross-validation repeat, showing the relationship between actual and predicted Total scores. .

sions are drawn.

4.3 RQ3: Generalization to an Independent Cohort (H3.1.)

I also sought to test whether a CPM model trained on a Japanese community sample would generalize to German participants from an independent community cohort. This required a reliable predictive model developed using the Japanese data that could then be applied, unchanged, to the German individuals. As reported in Section 4.1, however, the models showed no significant out-of-sample prediction during cross-validation. Therefore, Hypothesis 3.1 could not be tested as originally specified.

However, to see whether the null findings persisted across cohorts, I next ran the full CPM pipeline independently on the German dataset, using SD3 psychopathy subscale scores as the target variable for prediction. The results were similarly null, with cross-validated correlations between predicted and observed scores being near zero, permutation tests being non-significant, and mean absolute errors being comparable to a mean-prediction baseline (see Table 4.2). Null findings persisted even when restricting the age range to match the Japanese sample or when stratifying by sex, meaning resting-state functional connectivity did not significantly predict the

Table 4.2: German dataset — MAE and Pearson r (mean [sd] across CV repeats) with permutation p-values for *connectome* and *residuals*.

			MAE		Pearson r	
Target	**Model**	**Network**	**mean [sd]**	p	**mean [sd]**	p
All data	connectome	positive	3.77 [0.54]	0.157	0.13 [0.21]	0.128
		negative	3.83 [0.56]	0.238	0.01 [0.22]	0.473
		both	3.66 [0.53]	0.103	0.11 [0.22]	0.178
	residuals	positive	4.19 [0.64]	0.740	−0.09 [0.22]	0.796
		negative	4.27 [0.61]	0.848	−0.17 [0.21]	0.936
		both	4.32 [0.61]	0.937	−0.17 [0.20]	0.927
Youth only	connectome	positive	3.85 [0.59]	0.307	0.05 [0.22]	0.343
		negative	3.76 [0.62]	0.183	0.09 [0.22]	0.237
		both	3.66 [0.62]	0.171	0.10 [0.22]	0.236
	residuals	positive	4.06 [0.60]	0.561	−0.03 [0.20]	0.562
		negative	4.06 [0.65]	0.557	−0.04 [0.22]	0.628
		both	4.04 [0.63]	0.732	−0.05 [0.19]	0.641
Male	connectome	positive	3.76 [0.74]	0.094	0.14 [0.32]	0.166
		negative	4.52 [0.86]	0.936	−0.22 [0.26]	0.941
		both	3.98 [0.76]	0.562	−0.01 [0.29]	0.534
	residuals	positive	4.01 [0.85]	0.180	0.05 [0.34]	0.365
		negative	4.62 [0.94]	0.860	−0.21 [0.27]	0.931
		both	4.22 [0.88]	0.578	−0.09 [0.31]	0.726
Female	connectome	positive	3.47 [0.77]	0.777	−0.11 [0.34]	0.721
		negative	3.16 [0.72]	0.325	0.04 [0.36]	0.410
		both	3.20 [0.73]	0.569	−0.07 [0.35]	0.626
	residuals	positive	3.71 [0.82]	0.762	−0.13 [0.36]	0.757
		negative	3.41 [0.72]	0.417	0.02 [0.33]	0.451
		both	3.43 [0.76]	0.594	−0.08 [0.34]	0.668

severity of psychopathic traits.

4.4 RQ4 & RQ5: Alternative Model Implementations

I tested whether alternative modeling approaches, such as weighted-edge CPM and NBS+CPM, could improve performance over the baseline model. Neither implementation improved predictive accuracy relative to the baseline model. Test set Pearson's r values remained near zero for total and factor scores (see Table 4.3).

Table 4.3: Comparison of CPM variants using the combined edge set ("both") for connectome and residuals models (mean [sd] across CV repeats) with permutation p-values.

Target	Variant	Connectome				Residuals			
		MAE		Pearson r		MAE		Pearson r	
		mean [sd]	p	mean [sd]	p	mean [sd]	p	mean [sd]	p
Total	Baseline CPM	12.46 [1.64]	0.645	0.05 [0.23]	0.365	12.56 [1.72]	0.638	0.04 [0.23]	0.368
	Weighted-edge CPM	12.95 [1.69]	0.791	−0.04 [0.21]	0.633	13.08 [1.78]	0.808	−0.06 [0.22]	0.720
	NBS+CPM	12.31 [1.68]	0.593	0.08 [0.24]	0.277	12.34 [1.70]	0.601	0.08 [0.23]	0.283
Factor 1	Baseline CPM	7.87 [0.99]	0.799	0.03 [0.20]	0.396	7.84 [1.04]	0.692	0.06 [0.20]	0.333
	Weighted-edge CPM	8.14 [1.08]	0.866	−0.02 [0.20]	0.576	8.10 [1.12]	0.784	−0.01 [0.21]	0.535
	NBS+CPM	7.76 [1.00]	0.754	0.06 [0.22]	0.311	7.79 [1.01]	0.765	0.02 [0.21]	0.445
Factor 2	Baseline CPM	5.23 [0.80]	0.403	0.06 [0.27]	0.321	5.47 [0.81]	0.718	−0.01 [0.24]	0.524
	Weighted-edge CPM	5.32 [0.81]	0.388	0.03 [0.24]	0.385	5.54 [0.83]	0.671	−0.03 [0.24]	0.726
	NBS+CPM	5.18 [0.77]	0.367	0.08 [0.27]	0.243	5.17 [0.79]	0.339	0.09 [0.27]	0.235

4.5 RQ6: Sex Differences

To determine whether sex moderated predictive accuracy, I tested for sex differences in the primary models. I stratified the model by sex to test whether rsFC predicted total, Factor 1, or Factor 2 scores across males and females separately. The developed models did not yield significant results for either sex.

4.6 Post Hoc Analyses

The consistent null findings in my planned analyses (RQ1 - RQ6) motivated a set of further, unhypothesized analyses to understand potential reasons behind the null findings. I explored (a) whether a predictive signal existed at a more granular facet level and (b) whether the null results could be explained by data heterogeneity.

4.6.1 Antisocial Facet Predictive Signal

Given that CPM yielded null results for the total, Factor 1, and Factor 2 scores, I applied CPM to the four facets - interpersonal manipulation, callous effect, antisocial behavior, and erratic lifestyle - to investigate whether fine-grained dimensions would yield more precise findings. Among facet CPM models, only the antisocial behavior facet showed significant predictions on average across folds (see Table 4.4). The model based on positive network - edges whose connectivity strength was positively correlated with antisocial scores - showed modest but reliable performance (r = 0.27[0.24], p = 0.007**, MAE = 1.94[0.41]). A combined positive-plus-negative network model performed similarly (r = 0.27[0.31], p = 0.012*, MAE = 1.94[0.4]).

Table 4.4: CPM variants predicting antisocial behaviour facet: MAE, Pearson r, and R^2 (mean [sd] across CV repeats) with permutation p-values. Bold values indicate $p < .05$ (* $p < .05$, ** $p < .01$).

			MAE		**Pearson r**		R^2	
Model	**Modality**	**Network**	**mean [sd]**	p	**mean [sd]**	p	**mean [sd]**	p
CPM	connectome	positive	**1.94 [0.41]**	**0.005****	**0.27 [0.24]**	**0.007****	**-0.23 [0.53]**	**0.012***
		negative	2.13 [0.38]	0.109	0.16 [0.32]	0.073	**-0.31 [0.58]**	**0.031***
		both	**1.94 [0.40]**	**0.010****	**0.27 [0.31]**	**0.012***	**-0.15 [0.49]**	**0.009****
	residuals	positive	2.08 [0.40]	0.071	**0.20 [0.24]**	**0.038***	-0.35 [0.60]	0.056
		negative	2.18 [0.38]	0.189	0.14 [0.32]	0.111	-0.40 [0.67]	0.094
		both	2.04 [0.40]	0.072	**0.20 [0.30]**	**0.045***	-0.28 [0.61]	0.085
Weighted CPM	connectome	positive	**2.00 [0.43]**	**0.004****	**0.26 [0.26]**	**0.008****	**-0.26 [0.57]**	**0.006****
		negative	2.13 [0.41]	0.052	0.16 [0.27]	0.057	-0.39 [0.65]	0.051
		both	**1.98 [0.42]**	**0.007****	**0.25 [0.28]**	**0.008****	**-0.21 [0.54]**	**0.008****
	residuals	positive	**2.08 [0.44]**	**0.022***	**0.20 [0.26]**	**0.026***	**-0.35 [0.63]**	**0.023***
		negative	2.16 [0.42]	0.065	0.16 [0.28]	0.062	-0.44 [0.72]	0.069
		both	**2.06 [0.43]**	**0.030***	**0.21 [0.28]**	**0.024***	**-0.32 [0.63]**	**0.035***
NBS+CPM	connectome	positive	**1.96 [0.41]**	**0.007****	**0.27 [0.24]**	**0.009****	**-0.25 [0.56]**	**0.016***
		negative	2.18 [0.37]	0.252	0.14 [0.32]	0.109	-0.35 [0.60]	0.071
		both	**1.97 [0.40]**	**0.024***	**0.27 [0.31]**	**0.010****	**-0.16 [0.50]**	**0.017***
	residuals	positive	**2.03 [0.39]**	**0.035***	**0.23 [0.25]**	**0.020***	**-0.29 [0.56]**	**0.028***
		negative	2.18 [0.37]	0.213	0.15 [0.33]	0.092	-0.35 [0.62]	0.067
		both	2.00 [0.39]	0.052	**0.25 [0.31]**	**0.020***	**-0.19 [0.52]**	**0.033***

In contrast, the negative network did not pass the permutation testing (r = 0.16[0.32], p = 0.073, MAE = 2.13[0.38]). This effect was weaker but remained significant even when predicting the variance in antisocial behavior after regressing out covariates also produced significant but weaker correlations (pos.n.: r = 0.2[0.24], p = 0.038*, MAE = 1.94[0.41]; neg.n.: r = 0.14[0.32], p = 0.111, MAE = 2.18[0.38]; pos.n + neg.n.: r = 0.2[0.3], p = 0.045*, MAE = 2.04[0.4]). Furthermore, it was found that the alternative models (weighted CPM and NBS+CPM) offered no clear improvement for this one significant model. Cross-validated R^2 estimates were, on average, negative, reflecting that the predictions are close to a mean-prediction baseline. The details can be found in Table 4.4.

4.6.2 Networks Contributing to the Antisocial Facet Prediction

To identify which networks contributed the most to the antisocial behavior prediction, first, the edges that appeared in at least 80% of the 250 cross-validation folds were selected. From these stable predictive edges, I then computed node degree (hubness) for each ROI, defined as the number of stable predictive edges connected to each region, to quantify its contribution to the model. Regions with a higher degree therefore occurred in more of the most stable predictive connections. As shown in Figure 4.2, the positive network was dominated by hubs in the de-

fault mode network, followed by the control and salience networks. In contrast, the negative network showed the most prominent hubs in the control and default mode networks. Overall, the hub analysis revealed that both predictive networks, despite their opposite relationships to the antisocial score, converged on the same core systems: the default mode and frontoparietal control networks.

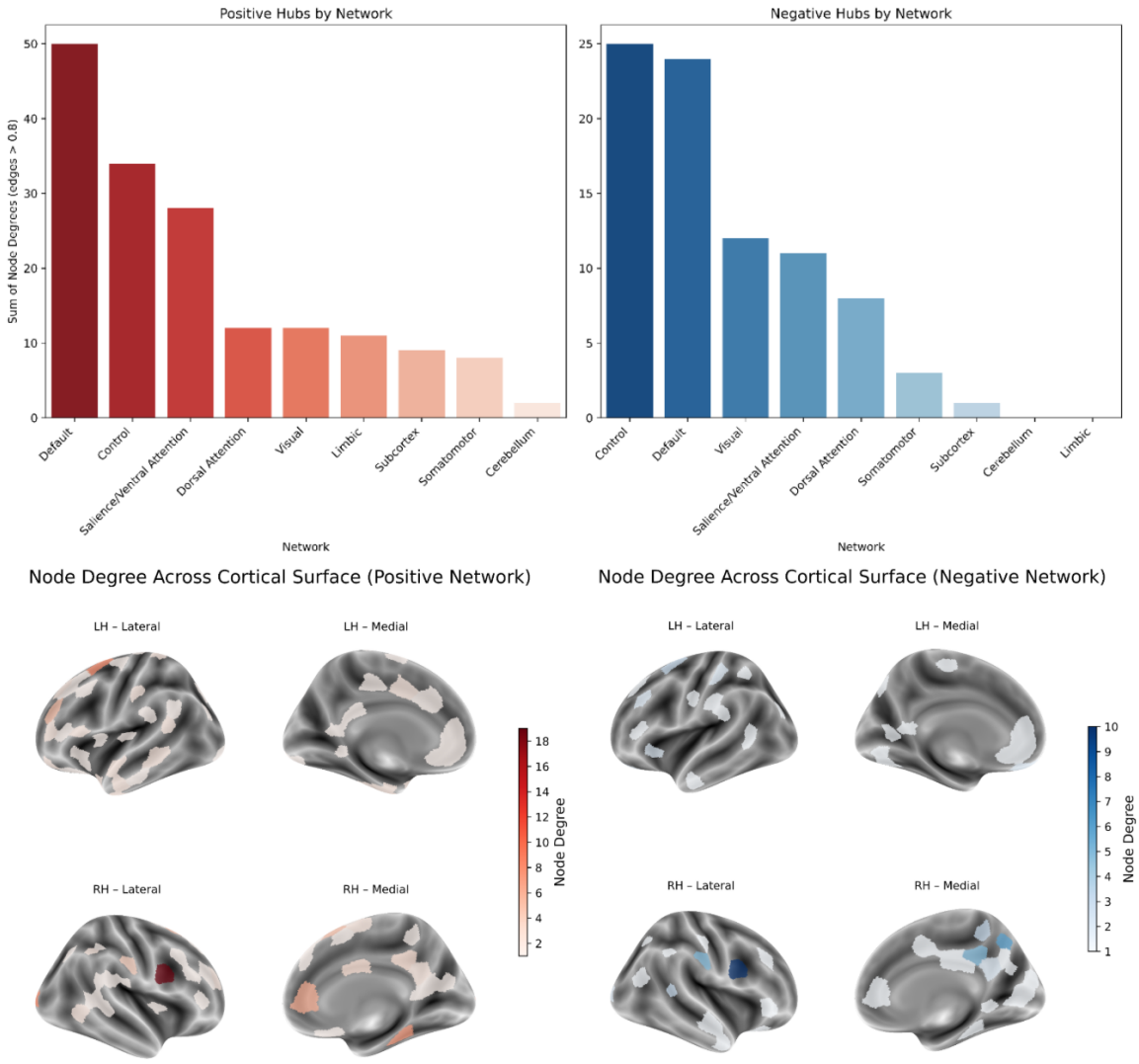

Figure 4.2: Networks Contributing to the Antisocial Facet Prediction.(a) Network-level and (b), (c) spatial distribution of stable predictive hubs for the antisocial behavior model.

4.6.3 Investigating Participants' Heterogeneity (IS-RSA)

Together, the results above suggest that the failure to predict psychopathy scores was not a simple artefact of the baseline pipeline, a peculiarity of the Japanese sample, or a product of unmodeled sex differences. These considerations motivated me to examine one of the possible explanations

in more detail: heterogeneity in the relationship between resting-state connectivity patterns and psychopathic traits across individuals.

To investigate whether the poor predictive performance of the CPM models corresponds to a high heterogeneity between brain connectivity and psychopathic traits, I employed inter-subject representational similarity analyses (IS-RSA).

Objectives

Recent work in resting-state fMRI has shown how meaningful individual differences can emerge in the pattern of similarity between participants. Particularly, inter-subject representational similarity analysis (IS-RSA) relates subject-by-subject neural similarity to subject-by-subject similarity in behavioral or trait measures[202], and has been used to uncover structure in affective experience[203], temperament[204], grit[205], and other personality traits[206, 207]. IS-RSA is therefore well-suited for asking whether the psychopathy continuum is reflected in the geometry of inter-individual connectivity patterns.

In post-hoc analyses, IS-RSA models were used to address the following questions:

- Do individuals with similar psychopathy scores show more similar functional connectivity patterns (Nearest-Neighbour (NN) model)?
- Do we observe an Anna Karenina (AnnaK) organization, where the brain connectivity of certain regions is especially similar at one extreme of the psychopathy continuum and increasingly diverges away from that extreme?
- Does using item-wise psychopathy profiles (rather than summary scores) strengthen brain-train coupling, as suggested by recent IS-RSA work[203] using item-level or high-dimensional behavioral representations?

All IS-RSA analyses were conducted at the parcel level. By testing how neural similarity matrices in the defined regions track different behavioral similarity models, these post-hoc analyses provided a follow-up to Hypothesis 2.1, and helped me to interpret why CPM prediction may have failed despite potential structure in the underlying connectivity-psychopathy relationship.

Nearest-Neighbor The first IS-RSA model tested whether individuals who are closer in Total psychopathic score also showed more similar functional connectivity patterns, irrespective of their absolute position on the trait continuum. Nearest-neighbor approach[202] treats psychopathy as a dimension along which both behavior and brain organization vary gradually.

For each region of interest, a neural similarity matrix was derived, that captured how similar

subjects' connectivity patterns are within that region. The behavioral similarity using the NN approach was defined as a monotonically decreasing function of absolute rank distance between individuals on the Total score on the SRP-SF scale. To quantify brain-behavior relationship under the NN hypothesis for each region, the neural and behavioral similarity patterns were correlated using a rank-based Spearman correlation. This procedure resulted into a single coefficient per parcel, where positive values indicate that in region *r*, pairs of subjects who are closer in total psychopathy score also tend to have similar FC.

Anna K The second IS-RSA model was Anna Karenina (AnnaK)[202], which tested the hypothesis that neural responses are especially similar at one extreme of the behavioral spectrum (here, psychopathic traits) and become more diverse toward the opposite end ("All high [or low] scorers are alike; each low [or high] scorer is different in their own way"). In contrast to the nearest-neighbor model, which emphasises relative distance along the scale (e.g., a pair of individuals scoring 1 and 10 are just as similar as individuals scoring 91 and 100), the AnnaK model encodes absolute position on the psychopathy continuum. In this thesis, the AnnaK model was used to test whether there are regions or networks in which high-psychopathy individuals show similar connectivity patterns, whereas lower-psychopathy individuals are more heterogeneous. Positive similarity values indicate that in a specific region, subjects towards the trait's higher extreme are more similar to one another than to individuals closer to the opposite end of the distribution.

Item-wise (Chen et al. (2020)) The NN and AnnaK models both encode one-dimensional behavioral scores; however, psychopathic traits are measured via multi-item questionnaires that capture a richer profile than any single total score. Recent IS-RSA work has shown that using item-wise response profiles to construct behavioral similarity matrices can substantially increase brain-behavior coupling compared with univariate scores. I therefore adopted Chen et al. (2020)[203] item-wise IS-RSA as a final approach to test whether local FC patterns track fine-grained psychopathy profiles. Positive brain-behavior similarity values indicate that subjects with more similar item-level psychopathy profiles also have more similar FC patterns in region *r*.

Results of IS-RSA

The Nearest Neighbors (NN) approach, testing whether subjects that are behaviorally similar are also nearby in the connectome space, revealed no regions showing significant correspon-

dence between similarity in psychopathy scores and brain connectivity. Parcel-wise rho values were concentrated around zero, suggesting that individuals with similar psychopathy levels do not share highly similar connectivity profiles. Additionally, none of the parcels survived false-discovery-rate (pFDR) correction (pFDR range: 0.93-0.99).

In contrast, the AnnaK approach, which tests the hypothesis that high-scoring individuals are neurally similar to each other, showed weak brain-behaviour similarity scores in regions of the default mode, salience/ventral attention, and frontoparietal control networks (see Figure 4.3). After FDR correction, parcel-wise pFDR values ranged from 0.65 to 0.99, and no parcel reached significance.

Finally, the item-wise approach (Chen et al., 2020), which aligns multivariate questionnaire patterns with neural similarity, suggests weak brain-behavior similarity scores that appear again in DMN, SN, and FPN (see Figure 4.3). FDR corrected p-values spanned 0.08-0.95, with no parcel surviving the correction.

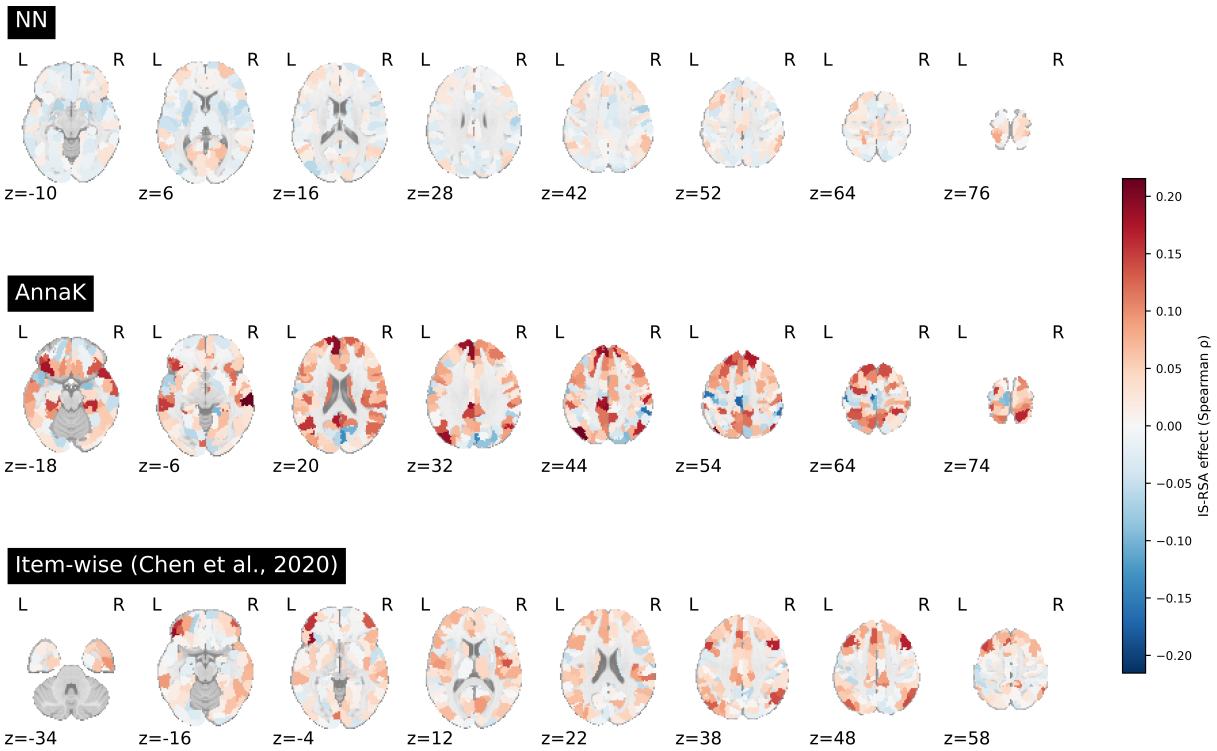

Figure 4.3: Whole-brain IS-RSA correlation maps for the NN, AnnaK, and item-wise (Chen et al. 2020) methods. Maps depict parcel-wise Spearman rho values representing the correspondence between neural similarity and behavioral similarity (measured by SRP-SF questionnaire) across subjects

To summarize the spatial trends, I performed network enrichment analyses of the top parcels exhibiting similar connectivity patterns in similar psychopathy levels (Fig. 4.4). Parcels belonging to default mode, salience, and frontoparietal control networks were overrepresented among the top-ranked regions, consistent with the patterns in the statistical maps (Fig. 4.3). Crucially,

however, none of the brain regions identified in any IS-RSA approach survived FDR correction, so the results should be interpreted with caution.

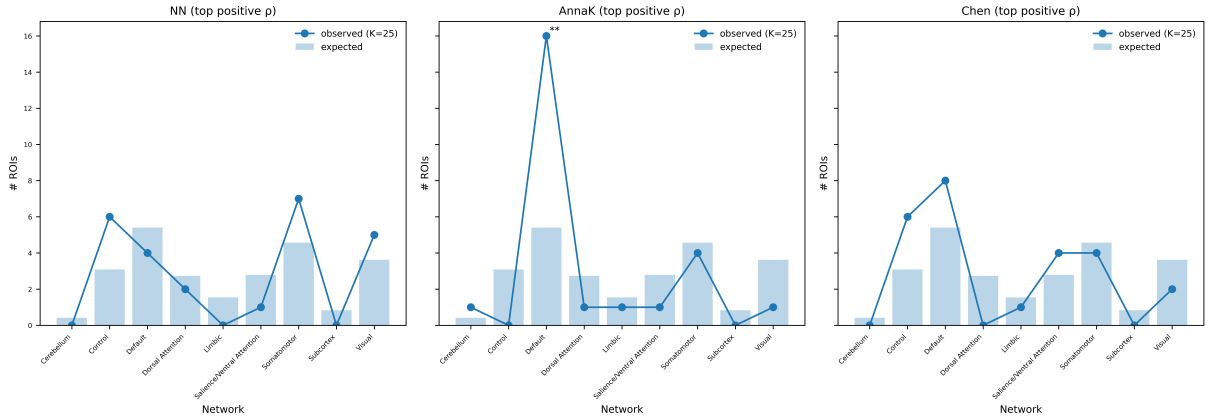

Figure 4.4: Network enrichment analysis of the top 25 positive IS-RSA regions across NN, AnnaK, and item-wise (Chen et al. 2020) methods. Blue lines represent the number of high-rho ROIs w.r.t. defined functional networks. Shaded bars reflect expected counts based on network size. Asterisks indicate networks with significant over-representation of top-25 parcels (* p $<$ .05, ** p $<$ 0.01, uncorrected)

As a final exploratory step, I investigated whether these spatial patterns aligned with previously reported functional networks. I computed the correlation between the parcel-wise IS-RSA effects and the "Psychopathy network" identified by Dugré and De Brito (2025). As shown in Figure 4.5, IS-RSA effects were positively, though weakly, correlated with the psychopathy network values ($r = 0.19$, $p < 0.001$).

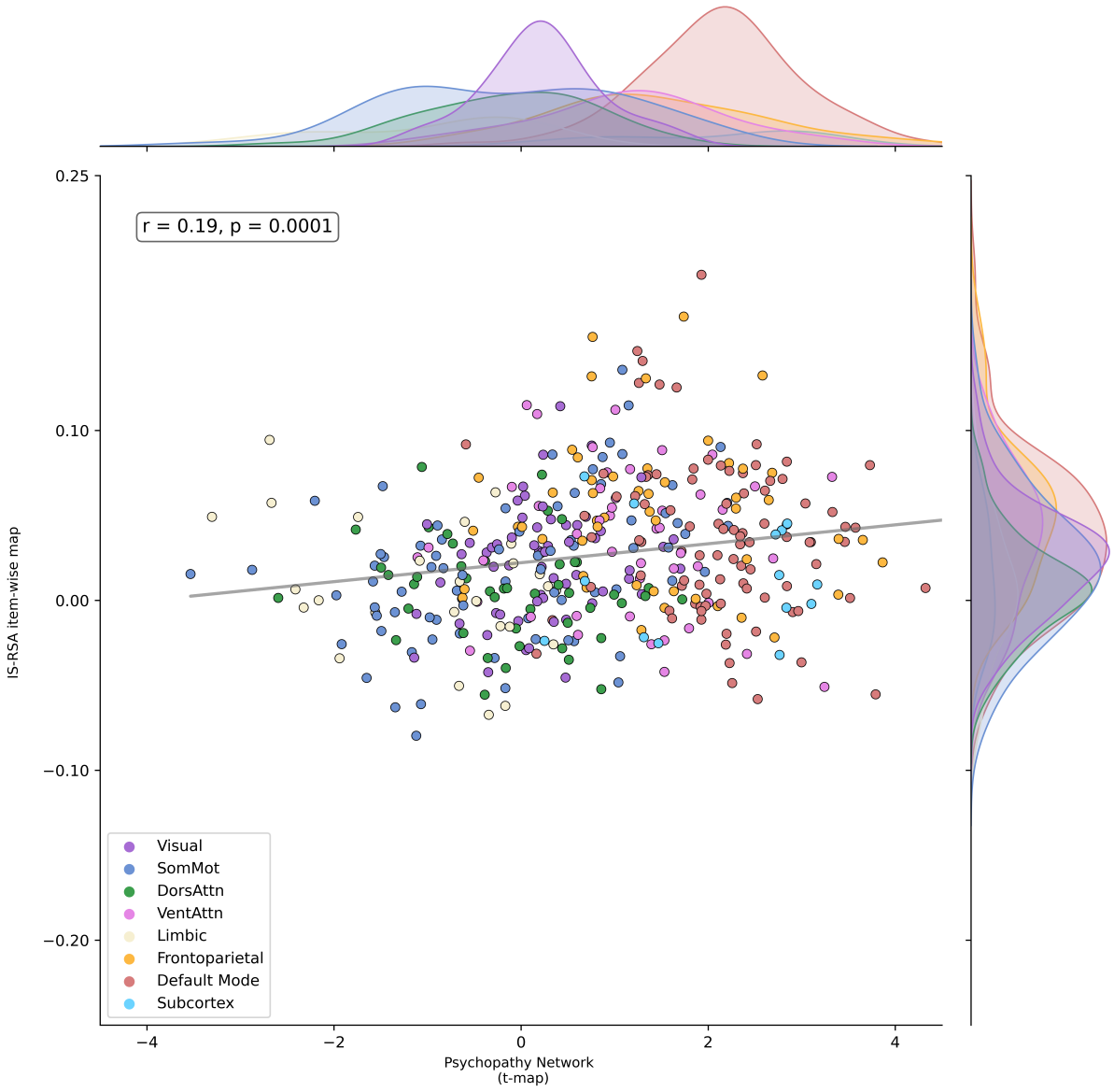

Figure 4.5: Correlation between parcel-wise IS-RSA (Chen et al., 2020) effects and the psychopathy network (Dugré et al., 2025). Each point represents a brain region colored by its assigned functional network.

5

Discussion

5.1 Overview of main findings

Over the past decades, neuroimaging studies have shown that individuals high in psychopathic traits often display altered brain structure and function[119, 156, 208]. Yet, most work has relied on relatively small, male-dominated forensic samples from the WEIRD population, leaving open the question of how replicable these brain-behavior associations are in community and non-Western populations. Against the established background, the present thesis investigated whether whole-brain resting-state functional connectivity can predict individual differences in psychopathic traits in community samples. Specifically, the primary aim was to test the predictive ability of functional connectivity in predicting psychopathic traits in a Japanese sample. Another goal was to identify which large-scale networks, if any, carry the predictive signal. Because most neuroimaging research in this field has been conducted in WEIRD samples, the study also explored cross-cultural generalization by testing the model on an independent German sample. As exploratory analyses, I also aimed to look into whether different aggregation or feature selection techniques might improve the model's performance (weighted CPM and NBS-CPM). Finally, the potential sex differences were investigated by applying the same modelling to females and males separately.

The results from these varied analyses offer several specific insights. Connectome-based predictive modeling did not yield a robust, generalizable predictive model for total and factor

scores in a Japanese sample. Since the predictive model could not be evaluated using the German dataset as initially planned, CPM was applied independently on the German dataset to see whether null findings persisted across cohorts. The null results from the primary dataset were also replicated in an external German dataset, indicating that the lack of strong resting-state FC association with the psychopathy traits was not limited to a single cultural group. Moreover, sex differences were not the reason for models' underperformance, as even after splitting the datasets into males vs females, no significant predictive signal was found. Additionally, neither weighted edge aggregation nor network-based statistics as a feature selection technique impacted the null results of the models. However, a modest effect was found between functional connectivity and the antisocial behavior facet of SRP-SF, where connections in default mode, salience, and frontoparietal networks contributed to the predictive signal.

Due to the consistent null findings throughout the hypothesized analyses, I performed a set of post-hoc analyses to understand the potential reasons behind the null results. Specifically, I utilized inter-subject representational similarity analysis to determine whether the psychopathic traits are reflected in the pattern of similarity between individuals' connectomes. The IS-RSA revealed weak correspondence between neural and behavioral similarity, concentrated primarily on the default mode, salience, and frontoparietal networks. Taken together, the results suggest that, while prior studies have shown that whole-brain connectivity may be a potential marker for psychopathy in a community sample[173], the relationship is rather complex.

5.2 Results in context with previous neuroimaging findings

Task-based and resting-state fMRI studies have linked psychopathy to altered activity and connectivity in a set of regions primarily encompassing default mode, salience, and frontoparietal networks, including the amygdala, hippocampus, ventromedial and dorsomedial prefrontal cortex, posterior cingulate/precuneus, insula, and striatum[44, 119, 209, 210]. In addition, a recent connectome-based predictive modelling study in Chinese college students[173] showed that whole-brain resting-state functional connectivity can predict individual differences in psychopathic traits, with predictive edges centered in anterior prefrontal, orbitofrontal, anterior cingulate, and insular cortices. Specifically, connectivity between the occipital network and the cingulo-opercular network emerged as the strongest predictor of individual differences in psychopathy severity[173].

Despite significant advances in unveiling the neurobiology of psychopathy, there is still no robust biomarker of psychopathy. Critical reviews have already highlighted that structural and

functional neuroimaging findings have been disparate, implicating a wide set of regions that are typically obtained from small samples, with diverse tasks and measurements[209, 210]. This brought researchers' attention to the inconsistent picture of neuroimaging findings in psychopathy. Koenigs et al., for instance, summarized functional MRI work showing that psychopathy is associated with abnormal activity across all four lobes and multiple subcortical regions, noting that "it is difficult to group the findings in any particular functional domain"[209]. Similarly, Pujol et al. synthesized anatomical and functional alterations in the brains of psychopathic individuals and emphasized that there are notable differences in the evidence provided by the existing studies, suggesting a possible biological heterogeneity of psychopathy[210].

More recent systematic reviews and meta-analyses have converged on a similar view. Johanson et al. (2020) reviewed 118 MRI neuroimaging studies (structural, diffusion, and functional) and concluded that although a default mode network consistently recurs across studies, the overall functional pattern is highly heterogeneous, with variability in which regions show associations and in which direction[119]. Deming and Koenigs (2020) task-fMRI meta-analysis identified increased task-related activity in midline cortical regions overlapping the default mode network and medial temporal lobe, alongside decreased activity in dorsal anterior cingulate cortex, which is a key salience network node. At the same time, their findings challenged amygdala hypoactivity and highlighted that consistent abnormalities are limited to a relatively small set of regions along with consistent variability elsewhere[44]. Finally, Deming et al. (2022) directly examined the amygdala findings and concluded that most MRI studies find null relationships between psychopathy and amygdala structure or function[43].

In the context of all the neuroscience works described above, the present findings fit the broader pattern depicted. Across all analyses, connectome-based predictive modelling did not yield stable predictive relationships for any psychopathy total, factor, or facet score. Even for the antisocial facet, which showed the strongest signal, cross-validated predictions were weak and did not outperform a simple mean-score baseline. Together, these findings suggest that resting-state connectivity associations with psychopathy levels in community samples are likely small and heterogeneous.

The null results obtained in this thesis can be interpreted within the context of brain-wide association studies (BWAS). Gratton et al. (2022) argue that human neuroscience has two realistic paths to reliable brain-behavior correlations. One is to maximize the sample size, and the other is to maximize the effect size through tightly targeted, within-subject designs[211]. In line with the first path, large multi-site work by Marek and colleagues (2022) has shown that correlations between whole-brain MRI measures and complex traits are much smaller than many

earlier single-site papers suggested. Additionally, replicable effects generally only emerge when sample sizes reach into the thousands. The study demonstrates that sample sizes in the tens or low hundreds tend to produce unstable effect sizes and poor replication[212]. From this perspective, having roughly 100 participants per cohort, the current study is well-powered by traditional imaging standards, but clearly underpowered for BWAS-scale effects. Under that assumption, developed CPM models trained on 100 individuals were unlikely to uncover a generalizable rsFC-behavior mapping, and the failure to predict SRP-SF total or factor scores above a mean baseline is explanatory. The second path outlined by Gratton et. al. is to maximize effect sizes through focused, high-precision investigations. Although the present study already targets a relatively specific phenotype in a community sample, the null findings suggest that rsFC-psycopathy associations are heterogeneous and not captured by a uniform connectivity pattern. This possibility motivated the use of IS-RSA, which is designed to target the brain-behavior relationships at the level of subject-to-subject similarity.

Finally, there are methodological reasons why CPM, as implemented in this study, may struggle to capture the brain-behavior relationships. CPM assumes a linear, additive mapping from edge weights to trait scores: each selected connection contributes independently and with a constant slope[167]. If the actual mapping is non-linear, depends on interactions between edges, or differs across groups, a linear model may not well approximate such relationships. The null CPM findings observed in this thesis underline the importance of future work investigating complementary non-linear approaches for prediction.

5.3 Post-hoc analyses

The null results obtained during prediction motivated me to explore the heterogeneity of the Japanese sample by using inter-subject representational similarity analysis. The nearest-neighbor model assumes that subjects close in the psychopathy continuum have similar functional connectivity patterns at particular regions. In a heterogeneous construct like psychopathy, where people with the same total score can have very different profiles (e.g., low on affective and high on interpersonal facets, and vice versa), this is a strong assumption. This study empirically shows that simply being close in total score does not imply closeness in the connectivity space.

Across the three IS-RSA variants, which each operationalized behavioral similarity in a different way, the clearest pattern emerged from the AnnaK model. This approach tests whether individuals with higher psychopathy scores show a more similar connectivity pattern to one another than would be expected by chance. In these post-hoc analyses, network enrichment suggested an

overrepresentation of default mode network edges, meaning that individuals at the higher end of psychopathy continuum share a slightly more similar DMN-centered organization compared to lower- or mid-scoring individuals. This finding broadly aligns with a recent resting-state study that combines person-specific network modelling with dimensional psychopathy measures. Dotterer et al. (2020) emphasize that the neural networks underlying psychopathic traits in young men are highly individualized overall, yet individuals with higher affective psychopathy features show increased density of connections between DMN and central executive networks[213].

A complementary perspective comes from the item-wise IS-RSA model, in which behavioral similarity was computed from the whole pattern of item responses rather than a single total score. Two individuals are considered similar if they endorse a similar configuration of responses across all SRP-SF questions, even if their overall scores differ. Interestingly, the model produced weak effects in default mode, salience, and control networks, and the resulting map showed the clearest correspondence with the "psychopathy network"(Dugré and De Brito, 2025[164]). The fact that item-wise IS-RSA yielded these results, where the NN model did not, could suggest that profile-level information across the spectrum carries a meaningful neural signal that is "washed out" when psychopathy is reduced to a single score. This fits with the broader argument that heterogeneity in psychopathy matters. Latzman et al.'s commentary on Poeppl et al.[118], for instance, explicitly warns that interpersonal-affective and impulsive-antisocial components show contrasting, sometimes opposing associations with behavioral and brain-based outcomes, and that global scores can obscure these effects[117].

5.4 Importance of considering culture

The replicability of null findings across culturally distinct samples highlights another key limitation of neuroimaging research. Most of what is currently known about the neural correlates of psychopathology comes from WEIRD samples[47]. At the same time, the cultural neuroscience literature shows that culture can reliably modulate neural responses in social and affective tasks[214, 215, 216]. Although a small number of neuroimaging studies have now examined psychopathic traits in non-Western samples[173, 217, 218, 219, 220], there is, to our knowledge, no systematic cross-cultural neuroimaging literature on psychopathy. As a result, there is no strong empirical basis to assume that psychopathy-brain mappings are identical across cultures. In this context, the present study contributes a modest first step by including two community samples from different cultural backgrounds (Japan and Germany). Both samples are drawn from relatively high-functioning, high-income populations, but they differ in cultural norms

and social context. These converging null results suggest that the main obstacle to predictive modelling might not be primarily cultural. Instead, the challenges identified earlier - very small effect sizes, heterogeneity of psychopathy as a phenotype, and the limitations of linear models - appear to apply broadly in similar ways to both Japanese and German adults. Taken together, these points highlight that, given our current state of knowledge, the primary challenge is to identify reliable neural correlates of psychopathic traits on a continuum before we can address finer-grained questions about cultural modulation.

5.5 Limitations

Several limitations of the present work should be acknowledged when interpreting the findings. First, although the sample sizes in both cohorts are typical for fMRI studies, large-scale analyses of brain-behavior relationships indicate that typical correlations between whole-brain functional connectivity and complex traits often require thousands of participants for stable, reproducible effects[211, 212]. Second, the CPM framework[167] used in the study also imposed several constraints. Following the original approach, CPM was implemented as a linear, additive model that does not take into consideration that brain-psychopathy relationships could be non-linear or could rely on higher-order interactions. Additionally, although the IS-RSA maps were aligned with prior network-level findings, most effects did not survive the correction for multiple comparisons and should therefore be considered with caution. Third, both samples used included individuals similar in socio-economic context. Thus, the results might not extend to culturally and socio-economically diverse groups. The results are also not extendable to adolescents or clinical/forensic populations with more extreme psychopathy scores. Finally, researchers must remain critical regarding the phenotyping of psychopathic traits, since both cohorts relied on self-report instruments (SRP-SF in Japan, SD3 psychopathy subscale in Germany), even though the evidence <ref from Background section> suggests that self-report questionnaires are a valid and reliable method for measuring psychopathic traits.

5.6 Future directions

These limitations point towards several promising avenues for future work. First, there is a need to study larger, richer, and more diverse samples. Multi-site datasets with thousands of participants, harmonised psychopathy measures, and coverage spanning community, clinical, and forensic samples would allow the field to move towards replicable and robust predictive

models. The ENIGMA Antisocial Behavior Working Group is one prominent initiative pursuing exactly this kind of large-scale, harmonized approach (ENIGMA-ASB; Thompson et al., 2020[221]). Second, considering the uncovered heterogeneity of psychopathy, future research would also benefit from individualized analyses. Specifically, working in the context of precision psychiatry, person-specific brain mapping could reveal functional estimates that are much more reliable and reveal robust features of network organization that are not visible in group-level data[222, 223]. Third, relatedly, functional connectome fingerprinting studies demonstrate that individuals can be reliably identified from their connectivity patterns alone[224], underscoring the strength of person-specific signatures in the functional connectome. Thus, incorporating within-individual analyses into studies of psychopathic traits may help to reveal meaningful individual differences in functional connectivity and to pinpoint neural correlates of psychopathy on an individual level.

Taken together, the results of this thesis suggest that resting-state functional connectivity does not currently provide a robust, generalizable predictive marker of psychopathic traits in community adults, at least in the Japanese and German samples studied here. Nonetheless, across CPM, IS-RSA and network-enrichment analyses, a picture emerged in which default mode, salience and frontoparietal networks appeared to carry the possible signal related to psychopathy, somewhat in line with previous literature. Methodologically, by combining connectome-based predictive modelling and inter-subject representational similarity approaches, and by reporting both null and exploratory findings, this thesis illustrates the limitations of resting-state functional connectivity as a predictive marker in psychopathy research. It also highlights the need to account for individual heterogeneity across the continuum and to move towards more individual-centered approaches as the next necessary step.

6

Conclusion

The present study was preregistered and conducted in line with current open-science recommendations (link). The thesis aimed to test whether whole-brain resting-state functional connectivity can account for individual differences in psychopathic traits in a community and whether such relationships generalize across two culturally distinct samples. Across both Japanese and German cohorts, resting-state functional connectivity did not yield a robust, generalizable predictive marker for psychopathy total, factor, and facets scores. At the same time, inter-subject similarity analyses suggested that connectivity profiles - in particular within default mode, salience, and frontoparietal control networks - are highly heterogeneous among individuals at the lower end of the psychopathy scale, which likely limits the ability of simple linear models to capture robust brain-behavior relationships. However, the results also showed that in community adults, the associations are null and not easily converted into accurate individual-level predictions. Finally, the thesis highlights both the value and the limitations of the utilized approaches. Predictive modelling can still uncover meaningful patterns in resting-state connectivity in relation to psychopathic traits, but the present results underscore the need for larger and more diverse samples, possibly more fine-grained psychopathy phenotyping, and more individual-centered frameworks. Together, this work clarifies what resting-state connectivity can realistically offer for predictive modelling and points towards more precision-oriented directions for future research.

References

[1] H. Cleckley, *The mask of sanity; an attempt to reinterpret the so-called psychopathic personality*, 5th ed. Mosby, 1976.

[2] S. A. De Brito *et al.*, "Psychopathy," *Nat. Rev. Dis. Primer*, vol. 7, no. 1, p. 49, 2021.

[3] B. Fox, "Psychopathic killers: A meta-analytic review of the psychopathy-homicide nexus," 2019.

[4] T. L. Nicholls, J. R. P. Ogloff, J. Brink, F. C. Psych, and A. Spidel, "Psychopathy in women: a review of its clinical usefulness for assessing risk for aggression and criminality," 2005.

[5] J.-P. Guay, "A taxometric investigation of psychopathy in women," 2018.

[6] A. Sanz-García, C. Gesteira, J. Sanz, and M. P. García-Vera, "Prevalence of psychopathy in the general adult population: A systematic review and meta-analysis."

[7] K. B. Werner, L. R. Few, and K. K. Bucholz, "Epidemiology, comorbidity, and behavioral genetics of antisocial personality disorder and psychopathy," *Psychiatr. Ann.*, vol. 45, no. 4, pp. 195–199, 2015.

[8] J. S. Sohn, A. Raine, and S. J. Lee, "The utility of the psychopathy checklist-revised (pcl-r) facet and item scores in predicting violent recidivism," *Aggress. Behav.*, vol. 46, no. 6, pp. 508–515, 2020.

[9] C. H. Allen *et al.*, "Psychopathy scores predict recidivism in high-risk youth: A five-year follow-up study," *Res. Child Adolesc. Psychopathol.*, vol. 52, no. 7, pp. 1089–1103, 2024.

[10] O. Vaurio, E. Repo-Tiihonen, H. Kautiainen, and J. Tiihonen, "Psychopathy and mortality," *J. Forensic Sci.*, vol. 63, no. 2, pp. 474–477, 2018.

[11] M. R. Donohue, C. P. Hoyniak, R. Tillman, D. M. Barch, and J. Luby, "Associations of observed callous–unemotional behaviors in early childhood with conduct problems and substance use over 14 years," *Dev. Psychopathol.*, vol. 35, no. 1, pp. 421–432, 2023.

[12] Z. Walsh, L. C. Allen, and D. S. Kosson, “Beyond social deviance: Substance use disorders and the dimensions of psychopathy,” *J. Personal. Disord.*, vol. 21, no. 3, pp. 273–288, 2007.

[13] A. Forth, S. Sezlik, S. Lee, M. Ritchie, J. Logan, and H. Ellingwood, “Toxic relationships: The experiences and effects of psychopathy in romantic relationships,” *Int. J. Offender Ther. Comp. Criminol.*, vol. 66, no. 15, pp. 1627–1658, 2022.

[14] D. T. Gatner, K. S. Douglas, M. F. E. Almond, S. D. Hart, and P. R. Kropp, “How much does that cost? examining the economic costs of crime in north america attributable to people with psychopathic personality disorder,” *Personal. Disord. Theory Res. Treat.*, vol. 14, no. 4, pp. 391–400, 2023.

[15] A. Newton, X. May, S. Eames, and M. Ahmad, “Economic and social costs of reoffending.”

[16] C. E. Rosenkilde, R. H. Bauer, and J. M. Fuster, “Single cell activity in ventral prefrontal cortex of behaving monkeys,” *Brain Res.*, vol. 209, no. 2, pp. 375–394, 1981.

[17] M. E. Leimkuhler and M.-M. Mesulam, “Reversible go–no go deficits in a case of frontal lobe tumor,” *Ann. Neurol.*, vol. 18, no. 5, pp. 617–619, 1985.

[18] S. J. Thorpe, E. T. Rolls, and S. Maddison, “The orbitofrontal cortex: Neuronal activity in the behaving monkey,” *Exp. Brain Res.*, vol. 49, no. 1, 1983.

[19] H. Damasio, T. Grabowski, and R. Frank, “The return of phineas gage: clues about the brain from the skull of a famous patient,” *Science*.

[20] J. L. Saver and A. R. Damasio, “Preserved access and processing of social knowledge in a patient with acquired sociopathy due to ventromedial frontal damage,” *Neuropsychologia*, vol. 29, no. 12, pp. 1241–1249, 1991.

[21] S. W. Anderson, J. Barrash, A. Bechara, and D. Tranel, “Impairments of emotion and real-world complex behavior following childhood- or adult-onset damage to ventromedial prefrontal cortex,” *J. Int. Neuropsychol. Soc.*, vol. 12, no. 2, pp. 224–235, 2006.

[22] J. Hiser and M. Koenigs, “The multifaceted role of the ventromedial prefrontal cortex in emotion, decision making, social cognition, and psychopathology,” *Biol. Psychiatry*, vol. 83, no. 8, pp. 638–647, 2018.

[23] D. T. Lykken, “A study of anxiety in the sociopathic personality,” *J. Abnorm. Soc. Psychol.*, vol. 55, no. 1, pp. 6–10, 1957.

[24] ——, *The Antisocial Personalities*, 1st ed. Psychology Press, 2013.

[25] C. J. Patrick, “Emotion and psychopathy: Startling new insights,” *Psychophysiology*, vol. 31, no. 4, pp. 319–330, 1994.

[26] C. M. Patterson and J. P. Newman, “Reflectivity and learning from aversive events: Toward a psychological mechanism for the syndromes of disinhibition,” *Psychol. Rev.*, vol. 100, no. 4, pp. 716–736, 1993.

[27] A. Baskin-Sommers and I. A. Brazil, “The importance of an exaggerated attention bottleneck for understanding psychopathy,” *Trends Cogn. Sci.*, vol. 26, no. 4, pp. 325–336, 2022.

[28] A. R. Damasio, “The somatic marker hypothesis and the possible functions of the prefrontal cortex,” *Philos. Trans. R. Soc. Lond. B. Biol. Sci.*, vol. 351, no. 1346, pp. 1413–1420, 1996.

[29] K. A. Kiehl, “A cognitive neuroscience perspective on psychopathy: Evidence for paralimbic system dysfunction,” *Psychiatry Res.*, vol. 142, no. 2–3, pp. 107–128, 2006.

[30] R. J. R. Blair, “Applying a cognitive neuroscience perspective to the disorder of psychopathy,” *Dev. Psychopathol.*, vol. 17, no. 3, pp. 865–891, 2005.

[31] A. Raine, T. Lencz, S. Bihrle, L. LaCasse, and P. Colletti, “Reduced prefrontal gray matter volume and reduced autonomic activity in antisocial personality disorder,” *ARCH GEN PSYCHIATRY*, vol. 57, 2000.

[32] A. Raine, M. S. Buchsbaum, J. Stanley, S. Lottenberg, L. Abel, and J. Stoddard, “Selective reductions in prefrontal glucose metabolism in murderers,” *Biol. Psychiatry*, vol. 36, no. 6, pp. 365–373, Sept. 1994.

[33] A. Raine, M. Buchsbaum, and L. LaCasse, “Brain abnormalities in murderers indicated by positron emission tomography.”

[34] K. A. K. et al., “Limbic abnormalities in affective processing by criminal psychopaths as revealed by functional magnetic resonance imaging,” *Biol. Psychiatry*, vol. 50, no. 9, pp. 677–684, Nov. 2001.

[35] M. C. C. et al., "Altered connections on the road to psychopathy," *Mol. Psychiatry*, vol. 14, no. 10, pp. 946–953, Oct. 2009.

[36] R. J. R. Blair, "Applying a cognitive neuroscience perspective to the disorder of psychopathy," *Dev. Psychopathol.*, vol. 17, no. 3, pp. 865–891, Sept. 2005.

[37] K. A. Kiehl, "A cognitive neuroscience perspective on psychopathy: Evidence for paralimbic system dysfunction," *Psychiatry Res.*, vol. 142, no. 2–3, pp. 107–128, June 2006.

[38] J. H. Kng, L. Luo, O. Choy, and J. Yu, "The intrinsic functional connectivity of psychopathy and its relation to self-control," *Biol. Psychol.*, vol. 194, p. 108979, Jan. 2025.

[39] P. Deming, C. J. Cook, M. E. Meyerand, K. A. Kiehl, D. S. Kosson, and M. Koenigs, "Impaired salience network switching in psychopathy," *Behav. Brain Res.*, vol. 452, p. 114570, Aug. 2023.

[40] C. H. A. et al., "Psychopathic traits and altered resting-state functional connectivity in incarcerated adolescent girls," *Front. Neuroimaging*, vol. 2, p. 1216494, Aug. 2023.

[41] M. Johanson, O. Vaurio, J. Tiihonen, and M. Lähteenvuo, "A systematic literature review of neuroimaging of psychopathic traits," *Front. Psychiatry*, vol. 10, p. 1027, Feb. 2020.

[42] P. Deming, S. Griffiths, J. Jalava, M. Koenigs, and R. R. Larsen, "Psychopathy and medial frontal cortex: A systematic review reveals predominantly null relationships," *Neurosci. Biobehav. Rev.*, vol. 167, p. 105904, Dec. 2024.

[43] P. Deming, M. Heilicher, and M. Koenigs, "How reliable are amygdala findings in psychopathy? a systematic review of mri studies," *Neurosci. Biobehav. Rev.*, vol. 142, p. 104875, Nov. 2022.

[44] P. Deming and M. Koenigs, "Functional neural correlates of psychopathy: a meta-analysis of mri data," *Transl. Psychiatry*, vol. 10, no. 1, p. 133, May 2020.

[45] M. L. Elliott, A. R. Knodt, and A. R. Hariri, "Striving toward translation: strategies for reliable fmri measurement," *Trends Cogn. Sci.*, vol. 25, no. 9, pp. 776–787, Sept. 2021.

[46] R. A. P. et al., "Scanning the horizon: towards transparent and reproducible neuroimaging research," *Nat. Rev. Neurosci.*, vol. 18, no. 2, pp. 115–126, Feb. 2017.

[47] C. Apicella, A. Norenzayan, and J. Henrich, "Beyond weird: A review of the last decade and a look ahead to the global laboratory of the future," *Evol. Hum. Behav.*, vol. 41, no. 5, pp. 319–329, Sept. 2020.

[48] E. Sterling, H. Pearl, Z. Liu, J. W. Allen, and C. C. Fleischer, "Demographic reporting across a decade of neuroimaging: a systematic review," *Brain Imaging Behav.*, vol. 16, no. 6, pp. 2785–2796, Dec. 2022.

[49] "Let's talk about diversity in human neuroscience," *Nat. Methods*, vol. 20, no. 8, pp. 1115–1115, Aug. 2023.

[50] H. H. Maung, "Psychopathic personalities and developmental systems."

[51] H. Cleckley, *The mask of sanity; an attempt to reinterpret the so-called psychopathic personality*. Mosby, 1941.

[52] R. D. Hare, "A research scale for the assessment of psychopathy in criminal populations," *Personal. Individ. Differ.*, vol. 1, no. 2, pp. 111–119, Jan. 1980.

[53] ——, *The Hare Psychopathy Checklist—Revised (PCL-R) Manual*, 2nd ed. Toronto, ON: Multi-Health Systems, 2003.

[54] G. F. et al., "Comparison between the psychopathy checklist-revised and the comprehensive assessment of psychopathic personality in a representative sample of spanish prison inmates," *PLOS ONE*, vol. 15, no. 2, p. e0228384, Feb. 2020.

[55] T. J. Harpur, A. R. Hakstian, and R. D. Hare, "Factor structure of the psychopathy checklist." *J. Consult. Clin. Psychol.*, vol. 56, no. 5, pp. 741–747, Oct. 1988.

[56] T. J. Harpur, R. D. Hare, and A. R. Hakstian, "Two-factor conceptualization of psychopathy: construct validity and assessment implications," *Psychological Assessment*, vol. 1, pp. 6–17, 1989, [Online]. Available: https://api.semanticscholar.org/CorpusID:143462043.

[57] R. D. Hare and C. S. Neumann, "Psychopathy as a clinical and empirical construct," *Annu. Rev. Clin. Psychol.*, vol. 4, no. 1, pp. 217–246, Apr. 2008.

[58] J. F. Edens, D. K. Marcus, S. O. Lilienfeld, and N. G. Poythress, "Psychopathic, not psychopath: Taxometric evidence for the dimensional structure of psychopathy." *J. Abnorm. Psychol.*, vol. 115, no. 1, pp. 131–144, Feb. 2006.

[59] J.-P. Guay, J. Ruscio, R. A. Knight, and R. D. Hare, "A taxometric analysis of the latent structure of psychopathy: Evidence for dimensionality." *J. Abnorm. Psychol.*, vol. 116, no. 4, pp. 701–716, Nov. 2007.

[60] K. M. Williams, D. L. Paulhus, and R. D. Hare, "Capturing the four-factor structure of psychopathy in college students via self-report," *J. Pers. Assess.*, vol. 88, no. 2, pp. 205–219, Mar. 2007.

[61] S. O. Lilienfeld and B. P. Andrews, "Development and preliminary validation of a self-report measure of psychopathic personality traits in noncriminal population," *J. Pers. Assess.*, vol. 66, no. 3, pp. 488–524, June 1996.

[62] C. Byworth, "Measuring personality constructs: The advantages and disadvantages of self-reports, informant reports and behavioural assessments."

[63] J. V. Ray, J. Hall, N. Rivera-Hudson, N. G. Poythress, S. O. Lilienfeld, and M. Morano, "The relation between self-reported psychopathic traits and distorted response styles: A meta-analytic review." *Personal. Disord. Theory Res. Treat.*, vol. 4, no. 1, pp. 1–14, 2013.

[64] S. A. Walker and C. MacCann, "Faking good and bad on self-reports versus informant-reports of dark triad personality," *Int. J. Sel. Assess.*, vol. 32, no. 3, pp. 329–342, Sept. 2024.

[65] N. G. Poythress *et al.*, "Using the pcl-r to help estimate the validity of two self-report measures of psychopathy with offenders," *Assessment*, vol. 17, no. 2, pp. 206–219, June 2010.

[66] C. J. Patrick, J. F. Edens, N. G. Poythress, S. O. Lilienfeld, and S. D. Benning, "Construct validity of the psychopathic personality inventory two-factor model with offenders." *Psychol. Assess.*, vol. 18, no. 2, pp. 204–208, June 2006.

[67] K. L. Lowman *et al.*, "Evaluating the validity of brief prototype-based informant ratings of triarchic psychopathy traits in prisoners," *Behav. Sci. Law*, vol. 39, no. 5, pp. 641–662, Oct. 2021.

[68] D. L. Paulhus, C. S. Neumann, R. D. Hare, K. M. Williams, and J. F. Hemphill, *Self-report Psychopathy Scale 4th Edition (SRP 4) Manual*. MHS, Multi-Health Systems Incorporated, 2017, [Online]. Available: https://books.google.co.uk/books?id=qkENvwEACAAJ.

[69] S. O. Lilienfeld, “Psychopathic personality inventory–revised.” 2016, sept. 12, 2016.

[70] C. J. Patrick and L. E. Drislane, “Triarchic model of psychopathy: Origins, operationalizations, and observed linkages with personality and general psychopathology,” *J. Pers.*, vol. 83, no. 6, pp. 627–643, Dec. 2015.

[71] M. R. Levenson, K. A. Kiehl, and C. M. Fitzpatrick, “Assessing psychopathic attributes in a noninstitutionalized population.” *J. Pers. Soc. Psychol.*, vol. 68, no. 1, pp. 151–158, 1995.

[72] D. K. Marcus, A. M. Lambros, M. G. Nagel, M. L. Ploe, K. L. Monaghan, and B. F. French, “Construction and preliminary validation of a psychopathic boldness scale in college and online samples.” *Psychol. Assess.*, vol. 37, no. 5, pp. 249–259, May 2025.

[73] D. R. Lynam, E. T. Gaughan, J. D. Miller, D. J. Miller, S. Mullins-Sweatt, and T. A. Widiger, “Assessing the basic traits associated with psychopathy: Development and validation of the elemental psychopathy assessment.” *Psychol. Assess.*, vol. 23, no. 1, pp. 108–124, 2011.

[74] D. N. Jones and D. L. Paulhus, “Introducing the short dark triad (sd3): A brief measure of dark personality traits.”

[75] C. S. Neumann and D. Pardini, “Factor structure and construct validity of the self-report psychopathy (srp) scale and the youth psychopathic traits inventory (ypi) in young men,” *J. Personal. Disord.*, vol. 28, no. 3, pp. 419–433, June 2014.

[76] M. K. Mahmut, C. Menictas, R. J. Stevenson, and J. Homewood, “Validating the factor structure of the self-report psychopathy scale in a community sample.” *Psychol. Assess.*, vol. 23, no. 3, pp. 670–678, Sept. 2011.

[77] K. V. Til, C. Vize, J. D. Miller, and D. R. Lynam, “Agreeableness explains the factor structure of the self-report psychopathy scale, fourth edition.” *Personal. Disord. Theory Res. Treat.*, vol. 13, no. 2, pp. 144–152, Mar. 2022.

[78] A. Seara-Cardoso, A. Queirós, E. Fernandes, J. Coutinho, and C. Neumann, “Psychometric properties and construct validity of the short version of the self-report psychopathy scale in a southern european sample,” *J. Pers. Assess.*, vol. 102, no. 4, pp. 457–468, July 2020.

[79] A. Seara-Cardoso, H. Dolberg, C. Neumann, J. P. Roiser, and E. Viding, "Empathy, morality and psychopathic traits in women," *Personal. Individ. Differ.*, vol. 55, no. 3, pp. 328–333, July 2013.

[80] K. M. Williams, D. L. Paulhus, and R. D. Hare, "Capturing the four-factor structure of psychopathy in college students via self-report," *J. Pers. Assess.*, vol. 88, no. 2, pp. 205–219, Mar. 2007.

[81] J. D. Miller and D. R. Lynam, "An examination of the psychopathic personality inventory's nomological network: A meta-analytic review." *Personal. Disord. Theory Res. Treat.*, vol. 3, no. 3, pp. 305–326, 2012.

[82] C. E. Sleep, B. Weiss, D. R. Lynam, and J. D. Miller, "An examination of the triarchic model of psychopathy's nomological network: A meta-analytic review," *Clin. Psychol. Rev.*, vol. 71, pp. 1–26, July 2019.

[83] A. Seara-Cardoso, A. Queirós, E. Fernandes, J. Coutinho, and C. Neumann, "Psychometric properties and construct validity of the short version of the self-report psychopathy scale in a southern european sample," *J. Pers. Assess.*, vol. 102, no. 4, pp. 457–468, July 2020.

[84] D. L. Paulhus and K. M. Williams, "The dark triad of personality: Narcissism, machiavellianism, and psychopathy," *J. Res. Personal.*, vol. 36, no. 6, pp. 556–563, Dec. 2002.

[85] S. N. Idris and M. Mahfar, "A conceptual paper of dark triad personality and cyberbullying issues among university students," *Int. J. Acad. Res. Bus. Soc. Sci.*, vol. 15, no. 6, pp. Pages 992–1003, June 2025.

[86] A. Somma, D. L. Paulhus, S. Borroni, and A. Fossati, "Evaluating the psychometric properties of the short dark triad (sd3) in italian adults and adolescents," *Eur. J. Psychol. Assess.*, vol. 36, no. 1, pp. 185–195, Jan. 2020.

[87] R. Čopková and L. Šafár, "Psychometric properties of the slovak version of short dark triad," *Eur. J. Investig. Health Psychol. Educ.*, vol. 11, no. 3, pp. 649–666, July 2021.

[88] A. Denovan, R. A. Plouffe, N. Dagnall, E. Artamonova, C. M. Kowalski, and D. H. Saklofske, "Dark triad, dyad, or core? a psychometric evaluation of the short dark triad (sd3) across three countries," *Curr. Psychol.*, vol. 43, no. 47, pp. 36 086–36 103, Dec. 2024.

[89] C. Wehner, U. Maaß, M. Leckelt, M. D. Back, and M. Ziegler, "Validation of the short dark triad in a german sample: Structure, nomological network, and an ultrashort version," *Eur. J. Psychol. Assess.*, vol. 37, no. 5, pp. 397–408, Sept. 2021.

[90] M. Malesza, P. Ostaszewski, S. Büchner, and M. C. Kaczmarek, "The adaptation of the short dark triad personality measure – psychometric properties of a german sample," *Curr. Psychol.*, vol. 38, no. 3, pp. 855–864, June 2019.

[91] Y. Rothemund *et al.*, "Fear conditioning in psychopaths: Event-related potentials and peripheral measures," *Biol. Psychol.*, vol. 90, no. 1, pp. 50–59, Apr. 2012.

[92] N. Birbaumer *et al.*, "Deficient fear conditioning in psychopathy: A functional magnetic resonance imaging study," *Arch. Gen. Psychiatry*, vol. 62, no. 7, p. 799, July 2005.

[93] R. Veit, L. Konicar, J. G. Klinzing, B. Barth, □. Yilmaz, and N. Birbaumer, "Deficient fear conditioning in psychopathy as a function of interpersonal and affective disturbances," *Front. Hum. Neurosci.*, vol. 7, 2013.

[94] K. Wilson, M. Juodis, and S. Porter, "Fear and loathing in psychopaths: a meta-analytic investigation of the facial affect recognition deficit," *Crim. Justice Behav.*, vol. 38, no. 7, pp. 659–668, July 2011.

[95] A. Dawel, R. O'Kearney, E. McKone, and R. Palermo, "Not just fear and sadness: Meta-analytic evidence of pervasive emotion recognition deficits for facial and vocal expressions in psychopathy," *Neurosci. Biobehav. Rev.*, vol. 36, no. 10, pp. 2288–2304, Nov. 2012.

[96] R. J. R. Blair, "The amygdala and ventromedial prefrontal cortex: functional contributions and dysfunction in psychopathy," *Philos. Trans. R. Soc. B Biol. Sci.*, vol. 363, no. 1503, pp. 2557–2565, Aug. 2008.

[97] P. Deming *et al.*, "Psychopathy is associated with fear-specific reductions in neural activity during affective perspective-taking," *NeuroImage*, vol. 223, p. 117342, Dec. 2020.

[98] J. P. Newman, C. S. Widom, and S. Nathan, "Passive avoidance in syndromes of disinhibition: Psychopathy and extraversion." *J. Pers. Soc. Psychol.*, vol. 48, no. 5, pp. 1316–1327, 1985.

[99] M. H. Thornquist and M. Zuckerman, "Psychopathy, passive-avoidance learning and basic dimensions of personality," *Personal. Individ. Differ.*, vol. 19, no. 4, pp. 525–534, Oct. 1995.

[100] R. Blair, "The emergence of psychopathy: Implications for the neuropsychological approach to developmental disorders," *Cognition*, vol. 101, no. 2, pp. 414–442, Sept. 2006.

[101] S. Gregory *et al.*, "Punishment and psychopathy: a case-control functional mri investigation of reinforcement learning in violent antisocial personality disordered men," *Lancet Psychiatry*, vol. 2, no. 2, pp. 153–160, Feb. 2015.

[102] M. Koenigs, M. Kruepke, J. Zeier, and J. P. Newman, "Utilitarian moral judgment in psychopathy," *Soc. Cogn. Affect. Neurosci.*, vol. 7, no. 6, pp. 708–714, Aug. 2012.

[103] Y. Gao and S. Tang, "Psychopathic personality and utilitarian moral judgment in college students," *J. Crim. Justice*, vol. 41, no. 5, pp. 342–349, Sept. 2013.

[104] E. M. Cardinale and A. A. Marsh, "Impact of psychopathy on moral judgments about causing fear and physical harm," *PLOS ONE*, vol. 10, no. 5, p. e0125708, May 2015.

[105] D. W. McRobbie, E. A. Moore, M. J. Graves, and M. R. Prince, *MRI from Picture to Proton*, 3rd ed. Cambridge University Press, 2017.

[106] G. H. Glover, "Overview of functional magnetic resonance imaging," *Neurosurg. Clin. N. Am.*, vol. 22, no. 2, pp. 133–139, Apr. 2011.

[107] B. M. Dale, M. A. Brown, and R. C. Semelka, *MRI Basic Principles and Applications*, 1st ed. Wiley, 2015.

[108] R. B. Buxton, "Interpreting oxygenation-based neuroimaging signals: the importance and the challenge of understanding brain oxygen metabolism," *Front. Neuroenergetics*, 2010.

[109] S. Ogawa, T. M. Lee, A. R. Kay, and D. W. Tank, "Brain magnetic resonance imaging with contrast dependent on blood oxygenation." *Proc. Natl. Acad. Sci.*, vol. 87, no. 24, pp. 9868–9872, Dec. 1990.

[110] N. K. Logothetis, J. Pauls, M. Augath, T. Trinath, and A. Oeltermann, "Neurophysiological investigation of the basis of the fmri signal," *Nature*, vol. 412, no. 6843, pp. 150–157, July 2001.

[111] M. D. Fox and M. E. Raichle, "Spontaneous fluctuations in brain activity observed with functional magnetic resonance imaging," *Nat. Rev. Neurosci.*, vol. 8, no. 9, pp. 700–711, Sept. 2007.

[112] S. A. H. Batouli and M. Sisakhti, "Some points to consider in a task-based fmri study: A guideline for beginners," *Front. Biomed. Technol.*, Apr. 2020.

[113] R. J. R. Blair, "Neuroimaging of psychopathy and antisocial behavior: A targeted review," *Curr. Psychiatry Rep.*, vol. 12, no. 1, pp. 76–82, Feb. 2010.

[114] A. Seara-Cardoso and E. Viding, "Functional neuroscience of psychopathic personality in adults," *J. Pers.*, vol. 83, no. 6, pp. 723–737, Dec. 2015.

[115] J. Decety, C. Chen, C. Harenski, and K. A. Kiehl, "An fmri study of affective perspective taking in individuals with psychopathy: imagining another in pain does not evoke empathy," *Front. Hum. Neurosci.*, vol. 7, 2013.

[116] L. M. Lenzen, M. R. Donges, S. B. Eickhoff, and T. B. Poeppl, "Exploring the neural correlates of (altered) moral cognition in psychopaths," *Behav. Sci. Law*, vol. 39, no. 6, pp. 731–740, Dec. 2021.

[117] R. D. Latzman, C. J. Patrick, and S. O. Lilienfeld, "Heterogeneity matters: implications for poeppl et al.'s (2019) meta-analysis and future neuroimaging research on psychopathy," *Mol. Psychiatry*, vol. 25, no. 12, pp. 3123–3124, Dec. 2020.

[118] T. B. P. et al., "A view behind the mask of sanity: meta-analysis of aberrant brain activity in psychopaths," *Mol. Psychiatry*, vol. 24, no. 3, pp. 463–470, Mar. 2019.

[119] M. Johanson, O. Vaurio, J. Tiihonen, and M. Lähteenvuo, "A systematic literature review of neuroimaging of psychopathic traits," *Front. Psychiatry*, vol. 10, p. 1027, Feb. 2020.

[120] B. Biswal, F. Z. Yetkin, V. M. Haughton, and J. S. Hyde, "Functional connectivity in the motor cortex of resting human brain using echo-planar mri," *Magn. Reson. Med.*, vol. 34, no. 4, pp. 537–541, Oct. 1995.

[121] M. E. Raichle, A. M. MacLeod, A. Z. Snyder, W. J. Powers, D. A. Gusnard, and G. L. Shulman, "A default mode of brain function," *Proc. Natl. Acad. Sci.*, vol. 98, no. 2, pp. 676–682, Jan. 2001.

[122] M. D. Fox, "Clinical applications of resting state functional connectivity," *Front. Syst. Neurosci.*, 2010.

[123] K. J. Friston, "Functional and effective connectivity in neuroimaging: A synthesis," *Hum. Brain Mapp.*, vol. 2, no. 1–2, pp. 56–78, Jan. 1994.

[124] S. B. Eickhoff, B. T. T. Yeo, and S. Genon, "Imaging-based parcellations of the human brain," *Nat. Rev. Neurosci.*, vol. 19, no. 11, pp. 672–686, Nov. 2018.

[125] A. S. et al., "Local-global parcellation of the human cerebral cortex from intrinsic functional connectivity mri," *Cereb. Cortex*, vol. 28, no. 9, pp. 3095–3114, Sept. 2018.

[126] J. D. P. et al., "Functional network organization of the human brain," *Neuron*, vol. 72, no. 4, pp. 665–678, Nov. 2011.

[127] M. Rubinov and O. Sporns, "Complex network measures of brain connectivity: Uses and interpretations," *NeuroImage*, vol. 52, no. 3, pp. 1059–1069, Sept. 2010.

[128] J. D. Power, K. A. Barnes, A. Z. Snyder, B. L. Schlaggar, and S. E. Petersen, "Spurious but systematic correlations in functional connectivity mri networks arise from subject motion," *NeuroImage*, vol. 59, no. 3, pp. 2142–2151, Feb. 2012.

[129] K. Murphy, R. M. Birn, and P. A. Bandettini, "Resting-state fmri confounds and cleanup," *NeuroImage*, vol. 80, pp. 349–359, Oct. 2013.

[130] O. E. et al., "fmriprep: a robust preprocessing pipeline for functional mri," *Nat. Methods*, vol. 16, no. 1, pp. 111–116, Jan. 2019.

[131] B. J. Seewoo, A. C. Joos, and K. W. Feindel, "An analytical workflow for seed-based correlation and independent component analysis in interventional resting-state fmri studies," *Neurosci. Res.*, vol. 165, pp. 26–37, Apr. 2021.

[132] E. Bullmore and O. Sporns, "Complex brain networks: graph theoretical analysis of structural and functional systems," *Nat. Rev. Neurosci.*, vol. 10, no. 3, pp. 186–198, Mar. 2009.

[133] J. S. D. et al., "Consistent resting-state networks across healthy subjects," *Proc. Natl. Acad. Sci.*, vol. 103, no. 37, pp. 13 848–13 853, Sept. 2006.

[134] S. M. S. et al., "Correspondence of the brain's functional architecture during activation and rest," *Proc. Natl. Acad. Sci.*, vol. 106, no. 31, pp. 13 040–13 045, Aug. 2009.

[135] V. Menon, "Large-scale brain networks and psychopathology: a unifying triple network model," *Trends Cogn. Sci.*, vol. 15, no. 10, pp. 483–506, Oct. 2011.

[136] P. N. A. et al., "An improved neuroanatomical model of the default-mode network reconciles previous neuroimaging and neuropathological findings," *Commun. Biol.*, vol. 2, no. 1, p. 370, Oct. 2019.

[137] M. E. Raichle, "The brain's default mode network," *Annu. Rev. Neurosci.*, vol. 38, no. 1, pp. 433–447, July 2015.

[138] J. R. Andrews-Hanna, J. Smallwood, and R. N. Spreng, "The default network and self-generated thought: component processes, dynamic control, and clinical relevance," *Ann. N. Y. Acad. Sci.*, vol. 1316, no. 1, pp. 29–52, May 2014.

[139] J. R. Andrews-Hanna, J. S. Reidler, J. Sepulcre, R. Poulin, and R. L. Buckner, "Functional-anatomic fractionation of the brain's default network," *Neuron*, vol. 65, no. 4, pp. 550–562, Feb. 2010.

[140] L. Q. Uddin, B. T. T. Yeo, and R. N. Spreng, "Towards a universal taxonomy of macro-scale functional human brain networks," *Brain Topogr.*, vol. 32, no. 6, pp. 926–942, Nov. 2019.

[141] L. Q. Uddin, "Salience processing and insular cortical function and dysfunction," *Nat. Rev. Neurosci.*, vol. 16, no. 1, pp. 55–61, Jan. 2015.

[142] W. W. Seeley, "The salience network: A neural system for perceiving and responding to homeostatic demands," *J. Neurosci.*, vol. 39, no. 50, pp. 9878–9882, Dec. 2019.

[143] J. L. Vincent, I. Kahn, A. Z. Snyder, M. E. Raichle, and R. L. Buckner, "Evidence for a frontoparietal control system revealed by intrinsic functional connectivity," *J. Neurophysiol.*, vol. 100, no. 6, pp. 3328–3342, Dec. 2008.

[144] S. Marek and N. U. F. Dosenbach, "The frontoparietal network: function, electrophysiology, and importance of individual precision mapping," *Dialogues Clin. Neurosci.*, vol. 20, no. 2, pp. 133–140, June 2018.

[145] T. A. Niendam, A. R. Laird, K. L. Ray, Y. M. Dean, D. C. Glahn, and C. S. Carter, "Meta-analytic evidence for a superordinate cognitive control network subserving diverse executive functions," *Cogn. Affect. Behav. Neurosci.*, vol. 12, no. 2, pp. 241–268, June 2012.

[146] M. W. Cole, J. R. Reynolds, J. D. Power, G. Repovs, A. Anticevic, and T. S. Braver, "Multi-task connectivity reveals flexible hubs for adaptive task control," *Nat. Neurosci.*, vol. 16, no. 9, pp. 1348–1355, Sept. 2013.

[147] J. Schimmelpfennig, J. Topczewski, W. Zajkowski, and K. Jankowiak-Siuda, "The role of the salience network in cognitive and affective deficits," *Front. Hum. Neurosci.*, vol. 17, p. 1133367, 2023.

[148] B. A. Seitzman, A. Z. Snyder, E. C. Leuthardt, and J. S. Shimony, "The State of Resting State Networks," *Top. Magn. Reson. Imaging*, vol. 28, no. 4, pp. 189–196, Aug. 2019.

[149] R. H. Kaiser, J. R. Andrews-Hanna, T. D. Wager, and D. A. Pizzagalli, "Large-Scale Network Dysfunction in Major Depressive Disorder: A Meta-analysis of Resting-State Functional Connectivity," *JAMA Psychiatry*, vol. 72, no. 6, p. 603, June 2015.

[150] L. Palaniyappan and P. F. Liddle, "Does the salience network play a cardinal role in psychosis? An emerging hypothesis of insular dysfunction," *J. Psychiatry Neurosci.*, vol. 37, no. 1, pp. 17–27, Jan. 2012.

[151] F. X. Castellanos and E. Proal, "Large-scale brain systems in ADHD: beyond the prefrontal-striatal model," *Trends Cogn. Sci.*, vol. 16, no. 1, pp. 17–26, Jan. 2012.

[152] B. T. T. Yeo *et al.*, "The organization of the human cerebral cortex estimated by intrinsic functional connectivity," *J. Neurophysiol.*, vol. 106, no. 3, pp. 1125–1165, Sept. 2011.

[153] A. A. Marsh *et al.*, "Reduced amygdala-orbitofrontal connectivity during moral judgments in youths with disruptive behavior disorders and psychopathic traits," *Psychiatry Res. Neuroimaging*, vol. 194, no. 3, pp. 279–286, Dec. 2011.

[154] J. C. Motzkin, J. P. Newman, K. A. Kiehl, and M. Koenigs, "Reduced Prefrontal Connectivity in Psychopathy," *J. Neurosci.*, vol. 31, no. 48, pp. 17 348–17 357, Nov. 2011.

[155] E. C. Finger *et al.*, "Impaired functional but preserved structural connectivity in limbic white matter tracts in youth with conduct disorder or oppositional defiant disorder plus psychopathic traits," *Psychiatry Res. Neuroimaging*, vol. 202, no. 3, pp. 239–244, June 2012.

[156] C. L. Philippi, M. S. Pujara, J. C. Motzkin, J. Newman, K. A. Kiehl, and M. Koenigs, "Altered Resting-State Functional Connectivity in Cortical Networks in Psychopathy," *J. Neurosci.*, vol. 35, no. 15, pp. 6068–6078, Apr. 2015.

[157] C. Korponay *et al.*, "Impulsive-Antisocial Dimension of Psychopathy Linked to Enlargement and Abnormal Functional Connectivity of the Striatum," *Biol. Psychiatry Cogn. Neurosci. Neuroimaging*, vol. 2, no. 2, pp. 149–157, Mar. 2017.

[158] ——, "Impulsive-antisocial psychopathic traits linked to increased volume and functional connectivity within prefrontal cortex," *Soc. Cogn. Affect. Neurosci.*, vol. 12, no. 7, pp. 1169–1178, July 2017.

[159] M. J. Jafri, G. D. Pearlson, M. Stevens, and V. D. Calhoun, "A method for functional network connectivity among spatially independent resting-state components in schizophrenia," *NeuroImage*, vol. 39, no. 4, pp. 1666–1681, Feb. 2008.

[160] F. A. Espinoza *et al.*, "Aberrant functional network connectivity in psychopathy from a large (N = 985) forensic sample," *Hum. Brain Mapp.*, vol. 39, no. 6, pp. 2624–2634, June 2018.

[161] ——, "Resting-state fMRI dynamic functional network connectivity and associations with psychopathy traits," *NeuroImage Clin.*, vol. 24, p. 101970, 2019.

[162] C. H. Allen *et al.*, "Aberrant resting-state functional connectivity in incarcerated women with elevated psychopathic traits," *Front. Neuroimaging*, vol. 1, p. 971201, Oct. 2022.

[163] "Psychopathy Checklist: Youth Version (PCL:YV)," in *The SAGE Encyclopedia of Criminal Psychology*. 2455 Teller Road, Thousand Oaks, California 91320: SAGE Publications, Inc., 2019.

[164] J. R. Dugré and S. A. D. Brito, "Mapping the psychopathic brain: Divergent neuroimaging findings converge onto a common brain network," *Neurosci. Biobehav. Rev.*, vol. 176, p. 106272, Sept. 2025.

[165] K. Smitha *et al.*, "Resting state fMRI: A review on methods in resting state connectivity analysis and resting state networks," *Neuroradiol. J.*, vol. 30, no. 4, pp. 305–317, Aug. 2017.

[166] J. R. Dugré and S. Potvin, "Impaired attentional and socio-affective networks in subjects with antisocial behaviors: a meta-analysis of resting-state functional connectivity studies," *Psychol. Med.*, vol. 51, no. 8, pp. 1249–1259, June 2021.

[167] X. Shen *et al.*, "Using connectome-based predictive modeling to predict individual behavior from brain connectivity," *Nat. Protoc.*, vol. 12, no. 3, pp. 506–518, Mar. 2017.

[168] M. D. Rosenberg *et al.*, “A neuromarker of sustained attention from whole-brain functional connectivity,” *Nat. Neurosci.*, vol. 19, no. 1, pp. 165–171, Jan. 2016.

[169] Z. Wang, K. S. Goerlich, H. Ai, A. Aleman, Y. Luo, and P. Xu, “Connectome-Based Predictive Modeling of Individual Anxiety,” *Cereb. Cortex*, vol. 31, no. 6, pp. 3006–3020, May 2021.

[170] H. Cao *et al.*, “A Functional Connectome-Based Neural Signature for Individualized Prediction of Antipsychotic Response in First-Episode Psychosis,” *Am. J. Psychiatry*, vol. 180, no. 11, pp. 827–835, Nov. 2023.

[171] M. Gao *et al.*, “Multimodal brain connectome-based prediction of suicide risk in people with late-life depression,” *Nat. Ment. Health*, vol. 1, no. 2, pp. 100–113, Feb. 2023.

[172] X. Wu *et al.*, “Connectome-based predictive modeling of compulsion in obsessive-compulsive disorder,” *Cereb. Cortex*, vol. 33, no. 4, pp. 1412–1425, Feb. 2023.

[173] S. Ye, B. Zhu, L. Zhao, X. Tian, Q. Yang, and F. Krueger, “Connectome-based model predicts individual psychopathic traits in college students,” *Neurosci. Lett.*, vol. 769, p. 136387, Jan. 2022.

[174] J. Tully, A. Frey, M. Fotiadou, N. J. Kolla, and H. Eisenbarth, “Psychopathy in women: insights from neuroscience and ways forward for research,” *CNS Spectr.*, vol. 28, no. 2, pp. 120–132, Apr. 2023.

[175] D. L. Paulhus, C. S. Neumann, and R. D. Hare, “Manual for the self-report psychopathy scale,” 2016.

[176] A. Babayan *et al.*, “A mind-brain-body dataset of MRI, EEG, cognition, emotion, and peripheral physiology in young and old adults,” *Sci. Data*, vol. 6, no. 1, p. 180308, Feb. 2019.

[177] N. Mendes *et al.*, “A functional connectome phenotyping dataset including cognitive state and personality measures,” *Sci. Data*, vol. 6, no. 1, p. 180307, Feb. 2019.

[178] S. Whitfield-Gabrieli and A. Nieto-Castanon, “Conn: A Functional Connectivity Toolbox for Correlated and Anticorrelated Brain Networks,” *Brain Connect.*, vol. 2, no. 3, pp. 125–141, June 2012.

[179] A. Nieto-Castanon, *Handbook of functional connectivity Magnetic Resonance Imaging methods in CONN*. Hilbert Press, 2020.

[180] J. L. R. Andersson, C. Hutton, J. Ashburner, R. Turner, and K. Friston, "Modeling Geometric Deformations in EPI Time Series," *NeuroImage*, vol. 13, no. 5, pp. 903–919, May 2001.

[181] K. J. Friston, J. Ashburner, C. D. Frith, J.-B. Poline, J. D. Heather, and R. S. J. Frackowiak, "Spatial registration and normalization of images," *Hum. Brain Mapp.*, vol. 3, no. 3, pp. 165–189, Jan. 1995.

[182] R. Henson, C. Büchel, O. Josephs, and K. Friston, "The Slice-Timing Problem in Event-related fMRI."

[183] R. Sladky, K. J. Friston, J. Tröstl, R. Cunnington, E. Moser, and C. Windischberger, "Slice-timing effects and their correction in functional MRI," *NeuroImage*, vol. 58, no. 2, pp. 588–594, Sept. 2011.

[184] S. Whitfield-Gabrieli, A. Nieto-Castanon, and S. Ghosh, "Artifact Detection Tools (ART)," 2011.

[185] J. D. Power, A. Mitra, T. O. Laumann, A. Z. Snyder, B. L. Schlaggar, and S. E. Petersen, "Methods to detect, characterize, and remove motion artifact in resting state fMRI," *NeuroImage*, vol. 84, pp. 320–341, Jan. 2014.

[186] A. Nieto-Castanon, "Preparing fMRI Data for Statistical Analysis."

[187] V. D. Calhoun *et al.*, "The impact of T1 versus EPI spatial normalization templates for fMRI data analyses," *Hum. Brain Mapp.*, vol. 38, no. 11, pp. 5331–5342, Nov. 2017.

[188] J. Ashburner and K. J. Friston, "Unified segmentation," *NeuroImage*, vol. 26, no. 3, pp. 839–851, July 2005.

[189] J. Ashburner, "A fast diffeomorphic image registration algorithm," *NeuroImage*, vol. 38, no. 1, pp. 95–113, Oct. 2007.

[190] S. M. L, C. Seguin, R. E. Smith, and A. Zalesky, "Connectome spatial smoothing (CSS): Concepts, methods, and evaluation," *NeuroImage*, vol. 250, p. 118930, Apr. 2022.

[191] A. Schaefer *et al.*, "Local-Global Parcellation of the Human Cerebral Cortex from Intrinsic Functional Connectivity MRI," *Cereb. Cortex*, vol. 28, no. 9, pp. 3095–3114, Sept. 2018.

[192] B. Fischl, D. H. Salat, and E. Busa, "Whole Brain Segmentation: Automated Labelling of Neuroanatomical Structures in the Human Brain," *Neuron*, vol. 33, pp. 341–355, Jan. 2002.

[193] B. T. T. Yeo *et al.*, "The organization of the human cerebral cortex estimated by intrinsic functional connectivity," *J. Neurophysiol.*, vol. 106, no. 3, pp. 1125–1165, Sept. 2011.

[194] K. Yoo *et al.*, "Connectome-based predictive modeling of attention: Comparing different functional connectivity features and prediction methods across datasets," *NeuroImage*, vol. 167, pp. 11–22, Feb. 2018.

[195] R. R. Wilcox and A. K. Barbey, "Connectome-based predictive modeling of fluid intelligence: evidence for a global system of functionally integrated brain networks," *Cereb. Cortex*, vol. 33, no. 19, pp. 10 322–10 331, Sept. 2023.

[196] H. Cai, J. Zhu, and Y. Yu, "Robust prediction of individual personality from brain functional connectome," *Soc. Cogn. Affect. Neurosci.*, vol. 15, no. 3, pp. 359–369, May 2020.

[197] Z. Ben-Zion *et al.*, "Connectome-Based Predictive Modeling of PTSD Development Among Recent Trauma Survivors," *JAMA Netw. Open*, vol. 8, no. 3, p. e250331, Mar. 2025.

[198] K. Ibrahim *et al.*, "Large-Scale Functional Brain Networks of Maladaptive Childhood Aggression Identified by Connectome-Based Predictive Modeling," 2021, in Review.

[199] D. Chyzhyk, G. Varoquaux, M. Milham, and B. Thirion, "How to remove or control confounds in predictive models, with applications to brain biomarkers," *GigaScience*, vol. 11, p. giac014, Mar. 2022.

[200] A. Zalesky, A. Fornito, and E. T. Bullmore, "Network-based statistic: Identifying differences in brain networks," *NeuroImage*, vol. 53, no. 4, pp. 1197–1207, Dec. 2010.

[201] E. Serin, A. Zalesky, A. Matory, H. Walter, and J. D. Kruschwitz, "NBS-Predict: A prediction-based extension of the network-based statistic," *NeuroImage*, vol. 244, p. 118625, Dec. 2021.

[202] E. S. Finn *et al.*, "Idiosynchrony: From shared responses to individual differences during naturalistic neuroimaging," *NeuroImage*, vol. 215, p. 116828, July 2020.

[203] P.-H. A. Chen, E. Jolly, J. H. Cheong, and L. J. Chang, "Intersubject representational similarity analysis reveals individual variations in affective experience when watching erotic movies," *NeuroImage*, vol. 216, p. 116851, Aug. 2020.

[204] Y. Qiu, X. Wu, B. Liu, R. Huang, and H. Wu, "Neural substrates of affective temperaments: An intersubject representational similarity analysis to resting-state functional magnetic resonance imaging in nonclinical subjects," *Hum. Brain Mapp.*, vol. 45, no. 7, p. e26696, May 2024.

[205] S. Park, D. Park, and M. J. Kim, "Similarity in functional connectome architecture predicts teenage grit," *Soc. Cogn. Affect. Neurosci.*, vol. 18, no. 1, p. nsad047, Oct. 2023.

[206] Z. Liu, J. Liu, and F. Cui, "Exploring individual differences in the impact of cognitive constraints on prosocial decision-making via intrinsic brain connectivity," *Brain Imaging Behav.*, Sept. 2025.

[207] Y. Tang, Y. Hu, J. Zhuang, C. Feng, and X. Zhou, "Uncovering individual variations in bystander intervention of injustice through intrinsic brain connectivity patterns," *NeuroImage*, vol. 285, p. 120468, Jan. 2024.

[208] R. J. R. Blair, "The neurobiology of psychopathic traits in youths," *Nat. Rev. Neurosci.*, vol. 14, no. 11, pp. 786–799, Nov. 2013.

[209] M. Koenigs, A. Baskin-Sommers, J. Zeier, and J. P. Newman, "Investigating the neural correlates of psychopathy: a critical review," *Mol. Psychiatry*, vol. 16, no. 8, pp. 792–799, Aug. 2011.

[210] J. Pujol, B. J. Harrison, O. Contreras-Rodriguez, and N. Cardoner, "The contribution of brain imaging to the understanding of psychopathy," *Psychol. Med.*, vol. 49, no. 1, pp. 20–31, Jan. 2019.

[211] C. Gratton, S. M. Nelson, and E. M. Gordon, "Brain-behavior correlations: Two paths toward reliability," *Neuron*, vol. 110, no. 9, pp. 1446–1449, May. 2022.

[212] S. Marek *et al.*, "Reproducible brain-wide association studies require thousands of individuals," *Nature*, vol. 603, no. 7902, pp. 654–660, Mar. 2022.

[213] H. L. Dotterer, L. W. Hyde, D. S. Shaw, E. L. Rodgers, E. E. Forbes, and A. M. Beltz, "Connections that characterize callousness: Affective features of psychopathy are associated with personalized patterns of resting-state network connectivity," *NeuroImage Clin.*, vol. 28, p. 102402, 2020.

[214] N. O. Rule, J. B. Freeman, and N. Ambady, "Culture in social neuroscience: A review," *Soc. Neurosci.*, vol. 8, no. 1, pp. 3–10, Jan. 2013.

[215] S. Han and Y. Ma, "A Culture-Behavior-Brain Loop Model of Human Development," *Trends Cogn. Sci.*, vol. 19, no. 11, pp. 666–676, Nov. 2015.

[216] Y. Zhu, L. Zhang, J. Fan, and S. Han, "Neural basis of cultural influence on self-representation," *NeuroImage*, vol. 34, no. 3, pp. 1310–1316, Feb. 2007.

[217] T. Osumi, T. Nakao, Y. Kasuya, J. Shinoda, J. Yamada, and H. Ohira, "Amygdala dysfunction attenuates frustration-induced aggression in psychopathic individuals in a non-criminal population," *J. Affect. Disord.*, vol. 142, no. 1–3, pp. 331–338, Dec. 2012.

[218] S. C. Chester, T. Ogawa, M. Terao, R. Nakai, N. Abe, and S. A. D. Brito, "Cortical and subcortical grey matter correlates of psychopathic traits in a Japanese community sample of young adults: sex and configurations of factors' level matter!" *Cereb. Cortex*, vol. 33, no. 9, pp. 5043–5054, Apr. 2023.

[219] S. C. Chester *et al.*, "White Matter Correlates of Psychopathic Traits in a Japanese Community Sample: Sex Matters!" *Eur. J. Neurosci.*, vol. 62, no. 1, p. e70177, July 2025.

[220] W. Pu, Q. Luo, Y. Jiang, Y. Gao, Q. Ming, and S. Yao, "Alterations of Brain Functional Architecture Associated with Psychopathic Traits in Male Adolescents with Conduct Disorder," *Sci. Rep.*, vol. 7, no. 1, p. 11349, Sept. 2017.

[221] P. M. Thompson *et al.*, "ENIGMA and global neuroscience: A decade of large-scale studies of the brain in health and disease across more than 40 countries," *Transl. Psychiatry*, vol. 10, no. 1, p. 100, Mar. 2020.

[222] E. M. Gordon *et al.*, "Individual-specific features of brain systems identified with resting state functional correlations," *NeuroImage*, vol. 146, pp. 918–939, Feb. 2017.

[223] ——, "Precision Functional Mapping of Individual Human Brains," *Neuron*, vol. 95, no. 4, pp. 791–807.e7, Aug. 2017.

[224] E. S. Finn *et al.*, “Functional connectome fingerprinting: identifying individuals using patterns of brain connectivity,” *Nat. Neurosci.*, vol. 18, no. 11, pp. 1664–1671, Nov. 2015.

Acknowledgments

First of all, I would like to express my sincere gratitude to my supervisors, Prof. Alessandra Bertoldo, Prof. Stéphane De Brito and Dr. Jules Dugré for all the support and guidance. Thank you to Centre for Human Brain Health at the University of Birmingham, for hosting me for 10 months to write my thesis. I thank SCAN Lab specifically, for being such a great community, for providing a safe space for young researchers and stimulating a healthy research environment.

Thank you to the University of Padova for being my home university for 3 long years. Thank you Padova, I liked you a lot.

I would like to thank my friends: Anna B. and Sofiya G., for supporting me during my rambling in our group chat; Nastia S. and Vlasta K., for being with me here in the UK, showing me what a true UK experience is. And to everyone else who I did not name here, since I am writing this last minute and have no memories whatsoever...

Many thanks go to my parents, who love me no matter what. Same goes to my grandparents and family. Unconditional love is one of the things I learned to value from you.

Huge thank you to my dearest boyfriend. You were by my side all this time, and you still are, every single day. I love you < 3

Finally, my heartfelt thanks go to Armed Forces of Ukraine. Without you, my home could have been already taken. Because of you I can live in peace. Because of you I can study abroad, I can travel, I can go home and have a place called ”home”.

I love you all!

Finally-finally, I want to thank myself, my body, my brain. It’s incredible, how may things we, people, can go through, and still be alive.